energy&fuels

pubs.acs.org/EF

Review

Chemical Looping for Combustion of Solid Biomass: A Review

Antonio Coppola and Fabrizio Scala*

Cite This: *Energy Fuels* 2021, 35, 19248−19265

Read Online

ACCESS | Metrics & More | Article Recommendations

ABSTRACT: Chemical looping combustion of solid biomass has the unique potential to generate energy with negative carbon emissions, while entailing an energy penalty compared to traditional combustion that is lower than that of the competing carbon capture technologies. In spite of these attractive features, research is still needed to bring the technology to a fully commercial level. The reason relies on a number of technological challenges mostly related to the oxygen carrier performance, its possible detrimental interaction with the biomass ash components, and the efficiency of the gas−solid contact with the biomass volatiles. This review is focused on these specific challenges which are particularly relevant when firing biomass rather than coal in a solid-based chemical looping combustion process. Special attention will be given to the most recent findings published on these aspects. Related performance evaluation by modeling, system integration, and techno-economic analysis will also be briefly reviewed.

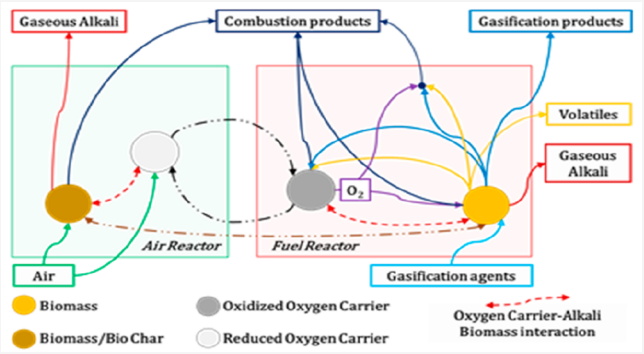

BACKGROUND ON CHEMICAL LOOPING COMBUSTION

Chemical Looping combustion (CLC) is a thermal fuel conversion technology with inherent CO_2 capture.[1] The core of CLC is the particulate solid oxygen carrier (OC), typically a metal oxide, which permits the fuel oxidation without direct contact between the fuel itself and the oxygen contained in the air. The CLC configuration entails two interconnected reactors named the fuel reactor (FR) and the air reactor (AR), respectively; in the FR the OC reacts with the fuel producing a flue gas mainly constituted by CO_2 and H_2O and the OC in its reduced form according to the schematic reaction R1. Thus, the fuel is converted with pure oxygen, resulting in a nitrogen-free flue gas. Continuously, the reduced OC is regenerated in the AR by air (eq R2).

$$\text{fuel} + Me_xO_y \rightarrow CO_2 + H_2O + Me_xO_{y-1} \quad \text{(R1)}$$

$$\text{air} + Me_xO_{y-1} \rightarrow Me_xO_y + O_2\ \text{depleted air} \quad \text{(R2)}$$

In the above lumped reaction scheme (R1 ± R2) Me_xO_y and Me_xO_{y-1} represent the oxidized and reduced form of the OC, respectively. A scheme of the CLC process is showed in Figure 1.

The concept of OC dates back to 1954 in a patent presented by Lewis and Gilliland[2] for the production of pure CO_2. Many years later, in 1983, Richter and Knoche[3] proposed a CLC configuration to improve the combustion efficiency of power plants. Ishida and co-workers[4] were the first to employ the name of chemical looping combustion for their studies on

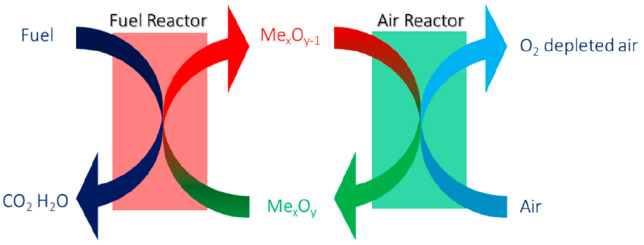

Figure 1. Scheme of the CLC process.

improving the exergy efficiency of natural gas power plants. From the same research group in 1994[5] the CLC process was proposed as a CO_2 capture system, also providing the first oxidation and reduction tests for OC in a thermogravimetric (TG) apparatus.[6] However, CLC was abandoned until 2000 when Lyngfelt and co-workers[1] proposed a two-interconnected fluidized bed scheme to evaluate the feasibility of CLC. Initially, CLC technology found its application in the framework of the carbon capture and storage (CCS) technologies as a CO_2 capture process from exploitation of fossil fuels. With respect to the competing technologies, such

Received: July 30, 2021
Revised: October 28, 2021
Published: November 11, 2021

as precombustion, postcombustion, and oxy-combustion, it presents a lower energy penalty.[7] Several authors[8−10] estimated the thermal efficiency of the CLC technology integrated with the integrated gasification combined cycle (IGCC) process, and the results highlighted a beneficial effect in terms of power production and CO_2 capture.

CLC was first demonstrated with gaseous fuels,[11] but also the application to liquid and solid fuels is feasible.[12] At present, the literature indicates that the total CLC operating experience amounts to over 11 000 h of operation in 49 CLC pilot reactors ranging in scale from 1.4 W_{th} to 10 MW_{th}.[13] Indeed, the TRL (Technology Readiness Level) of the technology is currently 6.[14] Whereas the application of CLC to gaseous fuel involves only typical problems relevant to gas−solid reactions, additional issues arise for liquid and solid fuels.[15,16] From a technical point of view, the main challenge of liquid-CLC is connected to the relative scarce experience in using liquid fuels in fluidized beds. In general, two different operating methods have been proposed: either the liquid is fully evaporated before feeding or it is directly injected in the reactor. On the other hand, the main problem related to the utilization of solid fuels is the solid−solid interaction with the OC. Different strategies have been suggested to overcome this limitation. Fuel gasification out of the CLC unit, followed by the introduction of syngas into the FR represents one of these strategies. However, this option, initially named ex-situ gasification chemical looping combustion (eG-CLC), is now definitively classified as gaseous fuel CLC, since the fuel is effectively fed to the FR in a gaseous phase.[12] The main disadvantages regarding this solution are the endothermic nature of the gasification step, the cost of the oxygen required for gasification, and the capital cost of the gasification reactor. Two alternative strategies are available which involve direct solid fuel feeding to the CLC system.[12] The first one consists of the direct gasification of the solid fuel inside the FR with a fraction of the CO_2 and H_2O recirculated from the outlet of the reactor. In this way, the produced syngas reacts with the OC inside the FR. This configuration is known as in situ gasification chemical looping combustion (iG-CLC). However, this configuration suffers from the escape of unconverted char particles to the AR, with the generation of uncaptured CO_2. A lumped kinetic scheme of iG-CLC in the FR is summarized below:[12]

$$\text{solid fuel} \rightarrow \text{char} + \text{volatile} \tag{R3}$$

$$\text{char} + \frac{CO_2}{H_2O} \rightarrow CO + H_2 + \text{ash} \tag{R4}$$

$$\text{volatiles, } CO,\ H_2 + Me_xO_y \rightarrow CO_2 + H_2O + Me_xO_{y-1} \tag{R5}$$

Another possibility was proposed by Mattisson et al. in 2009[17] based on the utilization of specific OCs able to release gaseous oxygen in the temperature range of interest for the CLC process. In this case, the released oxygen can directly react with the solid fuel. This process is called chemical looping with oxygen uncoupling (CLOU), which is also the name used to indicate the specific category of OCs adoptable for this purpose. The lumped reactions involved in the FR operated under CLOU mode are shown below:

$$Me_xO_y \rightarrow Me_xO_{y-1} + \frac{1}{2}O_2 \tag{R6}$$

$$\text{solid fuel} + O_2 \rightarrow CO_2 + H_2O + \text{ash} \tag{R7}$$

Obviously, the cornerstone for the success of the CLC technology is the performance of the OC. The majority of the operational experience so far—mostly obtained with gaseous fuels—relies on manufactured oxygen carriers based on Ni, Cu, Fe, or combined oxides.[13] More recently, an interest emerged for the combination of manganese with other oxides such as those of Fe, Ca, and Si, due to its CLOU properties. Specifically for solid fuels, the largest interest is focused on the utilization of cheap OCs, such as natural ores or waste materials.[18−20] The motivations must be sought in (i) the possible negative effect on the OC performance caused by the interaction with the solid fuel ash (the use of expensive OCs would not be recommended); (ii) the OC reactivity required for conversion of the gas derived from solid fuels (mainly H_2 and CO) is lower than that for conversion of more complex hydrocarbons; (iii) the obvious economic advantages of using cheap materials. A number of such materials have been demonstrated for their viability in CLC, which include ilmenite, iron ore, manganese ore, and $CaSO_4$-based oxygen carriers.[13]

CHEMICAL LOOPING COMBUSTION OF BIOMASS

In order to limit the effects of global warming, keeping a global temperature increase below 2 °C as settled in the Paris Agreement, the latest report from the Intergovernmental Panel on Climate Change (IPCC) established an indispensable change of the trend of CO_2 emissions.[21] Specifically, the CO_2 emission decrease should start in the present decade, and net negative CO_2 emissions should be reached by the end of the century. This scenario is the basis for the development of the so-called negative emission technologies (NETs), which allow the removal of CO_2 previously emitted into the atmosphere. Considering that an important fraction of CO_2 emissions is generated by the energy sector, among the NETs, only the use of bioenergy with carbon capture and storage (BECCS) would allow reaching this objective while heat and/or power are produced.[22,23]

In recent years, the use of biomass as the fuel in CLC (bio-CLC) has gained a great interest as a BECCS option, since both the costs and the energy penalty associated with this CO_2 capture process are among the lowest.[14] Since biomass is an almost CO_2 neutral fuel, a CLC system fueled with biomass implies that CO_2 would be effectively captured from the atmosphere. Although CLC with fossil-derived solid fuels has been demonstrated in various pilot plants, bio-CLC is a less explored area. Indeed, less than half of the pilot systems capable of using solid fuels have been operated using biomass.[12] Pröll and Zerobin[24] investigated biomass-based combined heat and power (CHP) generation with different carbon capture approaches. The results showed that bioenergy plants based on sustainably grown biomass can avoid a certain amount of CO_2 emissions through substitution of fossil fuels. In particular, the CLC technology promises significantly lower energy penalties compared to postcombustion CO_2 capture using gas−liquid absorption.

As explained previously, for the correct application to solid fuels of a CLC system either the fuel needs to be converted to gaseous species (i.e., iG-CLC) or the OC must release gaseous oxygen (i.e., CLOU). Moreover, it is worth highlighting that the composition of the solid fuel has a relevant effect on the overall process performance. Indeed, fossil-derived fuels tend to have a moderate content of volatiles and thus a large fraction of fixed carbon and ash. This implies that the rate

https://doi.org/10.1021/acs.energyfuels.1c02600
Energy Fuels 2021, 35, 19248−19265

Table 1. OCs Tested in CLC Operation with Biomass[a]

active oxide/support	fuel	operator	unit	time, h	ref
NiO/Al_2O_3 35/65	sawdust	Nanjing	10 kW	100	30
NiO/Al_2O_3 60/40	rice straw	Nanjing	25 kW	>7	31
$CuO/MgAl_2O_4$ 60/40	olive stone, sawdust, almond shell	CSIC	0.5/1.5 kW	10	32
CuO/γ-Al_2O_3	hardwood, lignite	Hamburg	25 kW	5	33
CuO on $MgAl_2O_4$ 60/40	sawdust	CSIC	0.5/1.5 kW	40	34
Cu−Mn mixed oxide	almond shell				
	olive stone				
CuO + iron ore	straw char	Xi'an	TGA	*b*	35
CuO + chrysolite					
CuO + limestone					
Fe_2O_3	sawdust	Nanjing	10 kW	30	36
Fe_2O_3/Al_2O_3 70/30	sawdust	Guangzhou	10 kW	60	37, 38
Fe_2O_3/Al_2O_3/NiO 7/3/0.53	sawdust	Guangzhou	10 kW	2	39
$CaMn_{0.9}Mg_{0.1}O_3$	wood char, petcoke	Chalmers	10 kW	74	40, 41
$Mn_3O_4/SiO_2/TiO_2$	wood char, coal, petcoke, lignite	Chalmers	10 kW	32	42
$Cu_{34}Mn_{66}$	olive stone, sawdust, almond shell	CSIC	0.5/1.5 kW	40	32
$CaMn_{0.78}Mg_{0.1}Ti_{0.12}O_3$ + ilmenite	black pellets	Chalmers	100 kW	18	43
	straw pellets				
	German wood char				
Fe ore	sawdust/coal	Nanjing	1 kW	*b*	44
Fe ore	sewage sludge	Nanjing	1 kW	10	45
Fe ore	sawdust	CSIC	0.5/1.5 kW	78	46
Fe ore	sawdust, olive stone, almond shell	CSIC	0.5/1.5 kW	40	47, 48
Fe ore	wood char, 2 coals	Chalmers	100 kW	26	49
Fe ore	rice husk	Nanjing	25 kW	>6	50
Fe ore	olive stone, sawdust	CSIC	50 kW	20	51
steel slag (Ca, Fe, Si, Mg, Mn)	wood char, wood pellets	Chalmers	10 kW	28	52
steel slag (Ca, Fe, Si, Mg, Mn)	wood char	Chalmers	300 W/10 kW	19.6	53
	wood pellets				
	steam-exploded wood pellets				
Fe ore	coal, torrefied biomass	Darmstadt	1 MW	42	54
Fe ore	sewage sludge	Nanjing	5 kW	8	55
Fe ore	sawdust	Nanjing	5 kW	3	56
	rice husk				
ilmenite	wood char	Chalmers	100 kW	12	57
ilmenite	wood char, petcoke	Chalmers	100 kW	34	58
ilmenite + Mn ore	wood char, 2 petcokes	Chalmers	100 kW	18	59
ilmenite	coal, lignite, biomass	Hamburg	25 kW	30	60
ilmenite	spruce trees	Chalmers	1.4/10 MW	61	61
ilmenite	wood pellets	VTT	20 kW	16	62
ilmenite	wood pellets	SINTEF	150 kW	5	63
ilmenite	wood pellets	Vienna UT	80 kW	20	64
ilmenite	Swedish wood char	Chalmers	100 kW	*b*	65
MFe_2O_4 (M = Cu, Ni, and Co)	sawdust	Wuhan	lab-scale fluidized bed	*b*	66
Mn ore ilmenite	black pellets	Chalmers	10 kW	42	67
	Swedish wood char				
	German wood char				
Mn ore	wood char, petcoke	Chalmers	10 kW	42	68
Mn ore	wood char, wood pellets, coal	Chalmers	10 kW	22	69
Mn ore	wood char, coal, petcoke, lignite	Chalmers	100 kW	52	70
Mn ore	wood char, wood pellets, coal	Chalmers	100 kW	33	69
Mn ore	wood pellets, wood char	VTT	20 kW	23	71
Mn ore	spruce trees	Chalmers	1.4/10 MW	32	61
Mn ore	black pellets	Chalmers	10 kW	42	67
	Swedish wood char				
	German wood char				
Mn ore	synthetic biomass volatiles, methane	Chalmers	300W	*b*	72
Mn ore	pine wood	CSIC	0.5 kW	63	73
	olive stones				
	almond shells				
$Mn_3O_4 + Fe_2O_3 + TiO_2$	pine wood	CSIC	0.5 kW	*b*	74

https://doi.org/10.1021/acs.energyfuels.1c02600
Energy Fuels 2021, 35, 19248−19265

Table 1. continued

[a]Data reprinted with permission from refs 12 and 13. [b]Not available.

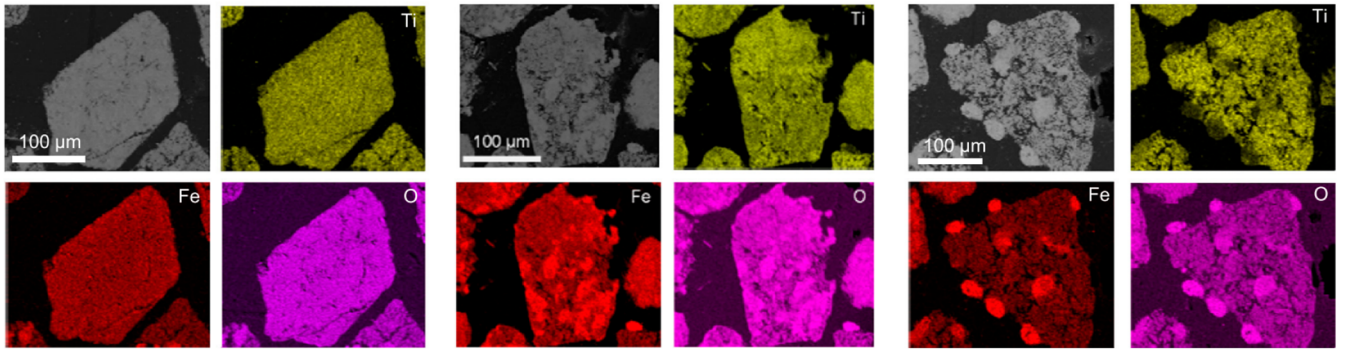

Figure 2. Elemental maps of Fe (red), Ti (yellow), and O (pink) on three representative particles of ilmenite varying in porosity and morphology. Measured porosity is increasing in the particles from left to right [Reprinted with permission from ref 65. Copyright 2015 Elsevier Ltd].

limiting step in a CLC process is the slow char gasification.[25,26] For biomass fuels, the situation is different since they have a much larger content of volatiles of about 60−85%.[27] This high volatile content together with the fact that devolatilization is a relatively fast process make more difficult an efficient contact between the volatiles fraction and the OC. Moreover, unlike char from fossil fuels, biochar conversion is typically not as slow since it is much more reactive. This feature is due to the high porosity and less ordered structure of biochar and to the larger content of alkali in the ash, such as Na and K, which have well-known catalytic activity.[28,29]

While comprehensive reviews on CLC have appeared in the recent literature,[12,13] in this review we focus on the specific challenges relevant to biomass combustion in a CLC process. As far as we know, such a review has not been reported before. The reasons behind these challenges, mostly related to the OC performance, the interaction between OC and biomass ash, and the efficiency of the gas−solid contact between OC and volatiles, will be discussed here in detail. Particular attention will be given to the most recent findings reported in the literature on these aspects. A final section will be devoted to performance evaluation, system integration, and techno-economic analysis related to bio-CLC. On the other hand, more general aspects common to all CLC systems will be not addressed in this review, and the reader is directed to the above comprehensive reviews to deepen his or her knowledge on such topics.

OXYGEN CARRIERS

The development of appropriate oxygen carriers is the crucial point for the success of CLC. In the past decade a lot of efforts have been made from the scientific community to find the best OCs. Many of these studies were focused on the application of CLC for gaseous, liquid, or solid fossil fuels, while only few were for bio-CLC, even if the trend is changing in the last years. A full collection of the different OCs tested for CLC, and their time of operation, is out of scope in this review and can be found in the recent reviews of Lyngfelt and co-workers.[12,13]

From the analysis of the latest literature focused on bio-CLC, it appears that most of the attention was devoted to low cost OCs, in particular from natural origin, mainly iron and manganese ores, but also waste materials from industry. Table 1 reports a collection of the different OCs tested with biomass so far.

In general, iron ores show low reactivity toward methane, but reasonable reactivity toward syngas. Among them, ilmenite $FeTiO_3$ (in reduced form), typically used for the extraction of TiO_2 in the pigment industry, shows an acceptable reactivity with syngas, which tends to increase with the number of cycles.

In one of the first works on bio-CLC, Shen and co-workers[36] investigated the CLC of pine sawdust with iron oxide in a 10 kW_{th} reactor under iG-CLC mode. They focused their attention on the effect of the FR temperature on the outlet gas composition from both FR and AR, the proportion of reacting biomass carbon and its conversion to CO_2 in the FR. The results showed that the biomass conversion to CO_2 decreases with the FR temperature, and this could be ascribable to the fact that CO production (from biomass gasification with CO_2) presents a stronger dependence on temperature than CO oxidation with the iron oxide OC. In other words, an increase in the FR temperature produced an increase of CO generation by biomass conversion, higher than its consumption by oxidation to CO_2. This provides evidence for the quite scarce reactivity of iron oxide as an OC. The X-ray analysis of the regenerated OC showed that there were no significant chemical species changes; only two phases were present Fe_2O_3 and Fe_3O_4 in the oxidized OC, while Fe_2O_3, FeO, and Fe were absent in the reduced OC, indicating that the Fe_2O_3 phase of the oxygen carrier was completely reduced to Fe_3O_4 by biomass syngas in the FR. Finally, the authors suggested to improve the conversion of biomass to CO_2 in the fuel reactor by adding a more reactive OC with higher oxygen ratio, such as a Ni-based OC.

On the same topic, it is worth citing the work of Wang et al.[66] These authors tried to use metal ferrites, MFe_2O_4 (M = Cu, Ni and Co) as OCs. These materials, prepared by sol−gel method, were tested in both TG and a lab-scale fluidized beds using pine sawdust as fuel. The best reactivity and lower initial reaction temperature were shown by $CuFe_2O_4$, followed by $CoFe_2O_4$ and $NiFe_2O_4$. Contrary to the utilization of iron oxide, both carbon conversion and carbon capture efficiency increased with increasing FR temperature. Carbon conversion was higher than 95%, and the carbon capture efficiency was around 94% for all the three ferrites investigated. XRD analysis revealed that $NiFe_2O_4$ was essentially decomposed into Ni and

https://doi.org/10.1021/acs.energyfuels.1c02600
Energy Fuels 2021, 35, 19248−19265

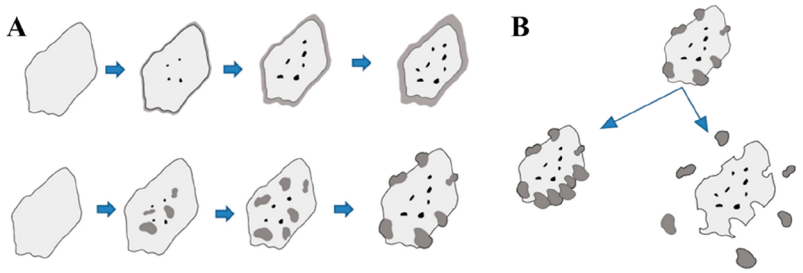

Figure 3. (A) Schematic illustration of the Fe migration in ilmenite exposed in a laboratory scale reactor (top) and in 100 kW reactor (bottom) with an increase of residence time. The dark gray areas represent areas with enrichment of Fe (Fe-segregation). The black areas represent formed pores. (B) Mechanism of structure development of ilmenite particles after long exposures and uneven iron segregation [Reprinted with permission from ref 65. Copyright 2015 Elsevier Ltd].

Fe_3O_4. Differently for $CuFe_2O_4$ which presented a reduced form mainly composed by Cu, $CuFeO_2$, and Fe_3O_4, for $CoFe_2O_4$ the reduction formed Co, FeO, and Fe_3O_4. These results were consistent with the thermodynamic analysis carried out by the same authors. Moreover, the presence of Cu and Co gave high thermal stability to the relative ferrites, and indeed, both carbon conversion and carbon capture efficiency remained at high values for five cycles. This was not true for $NiFe_2O_4$, whose performance decreased due to a severe sintering as confirmed by BET and SEM.

The possible positive effect related to the presence of other compounds in the Fe-based OCs is also clear with natural ores. Tierga ore from hematite mine in Tierga (Zaragoza, Spain) is mainly composed by Fe_2O_3, SiO_2, Al_2O_3, CaO, and MgO as revealed by XRD. This material showed a CO_2 capture of almost 100% without the use of a carbon stripper under specific conditions.[48] In particular, no differences in terms of combustion performance were observed among the biomass fuels (pine sawdust, olive stone, and almond shell). Both CO_2 capture efficiency and char conversion increased with the FR temperature. However, the high volatile content of biomass led to elevated requests of total oxygen demand, with values of about 25−30%. This was the case of olive stone that presents a higher volatile content. This was confirmed by specific tests using methane as a volatile reference compound and where the volatile conversion in these experiments was estimated to be about 70%.

Regarding ilmenite, the CLC tests confirmed that a layer rich in Fe was formed around a TiO_2 core (Figure 2). This phenomenon affected not only the particle surface but also the whole particle structure.[65] As a consequence, the particle morphology change entailed the formation of cracks and pores during the first stages, introducing shortcuts for oxygen. An Fe gradient was present at the particle edge and near the cracks and pores (Figure 3A), and this can be used as an indication of the residence time of the particles within the reactor. However, this Fe segregation determined a particle embrittlement (Figure 3B).

Manganese-based materials belong to the group of OCs which have the potential to give a CLOU effect. Manganese ores present different chemical compositions, which influence their performance as OCs. In these regards, Moldenhauer and co-workers[72] compared, in a lab-scale 300 W unit, the performance of five different manganese ores with synthetic biomass-volatiles composed by CO, H_2, CH_4, C_2H_4, and C_3H_6 and found that the different chemical composition had a significant effect on the OC chemical and mechanical stability.

Two of these ores (Elwaleed C and Guizhou) presented a high Fe/Mn ratio (4.41 and 1.59, respectively) and both showed good fuel conversion. However, for Elwaleed C a low chemical and mechanical stability was found, while Guizhou was the best ore, among those investigated, because it presented a good compromise between low attrition and good reactivity. Also Tshipi ore, a natural material with a more elevated content of Ca (Ca/Mn = 0.35) than the others, showed a good fuel conversion but the lowest lifetime under continuous redox conditions among the investigated materials. Probably, the combination of Mn and Fe, in particular in the form of bixbyite ($(Mn,Fe)_2O_3$), for the release of oxygen as well the presence of Ca seem to be beneficial in terms of reactivity.

The role of bixbyite was also highlighted in the work of Pérez-Astray et al.[74] They tested a synthetic OC composed by 60 wt % of Mn_3O_4, 33 wt % of Fe_2O_3, and a 7 wt % of TiO_2 ($(Mn_{66}Fe)$-Ti_7); the addition of TiO_2 led to an improvement of the oxygen uncoupling capability, reactivity, mechanical strength, and magnetic properties of the OC. The total oxygen demand (which represents the theoretical ratio of O_2 required for complete oxidation of residual gaseous combustibles from the FR) in the process decreased when the conversion of the spinel phase to bixbyite in the AR was increased and hence the oxygen release in the FR. The effective air excess ratio in the AR was the most significant variable for the bixbyite regeneration. Optimal conditions suggested values of about 3.0−3.2 for the air excess ratio in the AR with a temperature of around 880 °C, which ensured a spinel conversion to bixbyite of about 70% and a decrease of the total oxygen demand to values close to 10%.

However, the reasons of the differences in terms of chemical and mechanical stability are not yet clear. It is probable that dissimilarities in morphological features as well as the presence of other elements play a significant role. As a matter of fact, the Guizhou ore has a significant amount of Al, which led to an increase of the mechanical and chemical stability. Conversely, a relative high content of Ca might be a booster for sintering. The manganese ore, Morro da Mina ore, showed the lowest fuel conversion properties, which might be related to its nearly negligible oxygen release properties, related to its elevated content of Si and hence of braunite (Mn_7SiO_{12}), which tends to decompose during redox operation.

Braunite ore, with respect to Morro da Mina, exhibited a fair reactivity toward biomass volatiles despite the presence of Mn_7SiO_{12}. Probably, this is related to a lower content of Si. Its performance might be improved by fluid dynamic "tricks" such as increasing the gas velocity in the riser or using higher solid

https://doi.org/10.1021/acs.energyfuels.1c02600
Energy Fuels 2021, 35, 19248−19265

Table 2. List of Works Focused on OC−Ash Interaction

oxygen carriers	biomass/ash/pseudo-ash	experimental setup	OC−ash analysis methods	ref
Mn_3O_4−SiO_2	$CaCO_3$, K_2CO_3	fixed bed	XRD	89
Mn_3O_4−SiO_2−TiO_2	$CaHPO_4$		SEM-EDX	
Mn_3O_4−Fe_2O_3				
Mn_3O_4−Fe_2O_3−Al_2O_3				
hematite 84.0% $Fe_2O_3$16.0% Fe_3O_4	$CaCO_3$	fixed bed	XRD	90
hausmannite 93.7% Mn_3O_4 6.3% MnO	K_2CO_3			
synthesized ilmenite 87.6% Fe_2TiO_5	SiO_2			
12.4% TiO_2				
synthetic calcium manganite perovskite material and natural ilmenite	BP (pelletized steam-exploded stem wood)	two interconnected circulating fluidized beds (100 kW)	surface ionization detector (to detect alkali release in the CLC system)	43
	BP + K_2CO_3			
	BP + straw pellets			
	German wood char			
ilmenite	wood pellets	two interconnected circulating fluidized beds (60 kWth)	surface ionization detector (to detect alkali release in the CLC system)	91
braunite	wood char			
	straw pellets			
ilmenite	black pellets (BP, pelletized steam-exploded stem wood)	two interconnected circulating fluidized beds (10 kW)	surface ionization detector (to detect alkali release in the CLC system)	92
	Swedish wood char			
	German wood char			
	pine forest residue			
	straw pellet mix			
Fe_2O_3	Guanyun coal ash, tree ash	fixed bed	XRD	93
	straw ash	fluidized bed	XRF	
	pepper stalk ash		SEM-EDS	
Fe_2O_3	synthetic ash:	tube furnace	XRD	94
Fe_3O_4	SiO_2 31% (wt)		SEM-EDS	
	CaO 30%			
	K- and/or Na-based oxides 25%			
	MgO 6%			
	Al_2O_3 4%			
	Fe_2O_3 2%			
	MnO and TiO_2 2%			
ilmenite	K_2CO_3	fluidized bed	XRD	95
	KCl		BET surface area	
	KH_2PO_4		DTA-TGA	
	K_2SO_4			
iron ore	corn stalk ash	fixed bed	XRD	82
	rape stalk ash		BET	
	wheat straw ash			
iron ore	wheat stalk ash	fluidized bed	flue gas analysis	96
	corn stalk ash			
	soybean stalk ash			
LD-slag iron mill scale (Glödskal B)	KCl	tube furnace	XRD	97
	K_2CO_3 K_2SO_4		SEM-EDS	
	KH_2PO_4			
Fe_2O_3	high ash coal	fixed bed	flue gas analysis	98
	rice straw			

circulation rates. This was also confirmed in the work of Mei et al.:[67] an increase of the FR temperature and of the solids circulation generally had positive effects on the combustion performance, but a too high circulation decreased the carbon capture efficiency. Another option to reduce the oxygen demand was proposed by Pérez-Astray et al.[73] who suggested recycling the gas outlet stream into the FR. Simulations indicated that it is possible to reduce the oxygen demand up to 30% if working with manganese ores. Also, the fuel power input showed some effects on the process performance, the oxygen demand varied in the range of 2.6−38.4% and decreased with an increase of the FR temperature. In general, the oxygen demand with manganese ore decreased by 8−10% with respect to ilmenite. The estimated lifetime of the manganese ore particles is in the range of 200−830 h[67,69] which is at a comparable level to that of ilmenite.

Probably, Cu-based OCs are the most popular CLOU OCs, and many papers can be found in the literature using fossil fuels as feeding material. The CLOU effect makes Cu-based OCs quite attractive for bio-CLC. However, their elevated cost remains one of the main drawbacks. In comparison, Mn-based oxides present a slower oxygen release and greater thermodynamic restrictions associated with a lower operating temperature window than Cu-based oxides. However, mixed oxides

https://doi.org/10.1021/acs.energyfuels.1c02600
Energy Fuels 2021, 35, 19248−19265

based on Cu−Mn have shown high CLOU capability.[75] Adánez-Rubio and co-workers[32,34] tested two Cu−Mn mixed oxides with different types of biomass (pine sawdust, olive stones, and almond shells) in a continuous 1.5 kW_{th} CLC unit. The first OC, named $Cu_{34}Mn_{66}$, was composed by 34 wt % CuO and 66 wt % Mn_3O_4—active phase $Cu_{1.5}Mn_{1.5}O_4$—and the second one, named $Cu_{60}MgAl$, consisting of CuO (60 wt %) as the active phase and $MgAl_2O_4$ as the support. The authors detected combustion efficiency in the FR of 100% for both OCs and all biomasses. It is interesting to note that the relation between the CLOU effect and temperature for $Cu_{60}MgAl$ and $Cu_{34}Mn_{66}$ was different, and therefore, different operating windows for biomass combustion were determined. Thus, the CO_2 capture efficiency for pine sawdust reached 98% at 850 °C for $Cu_{34}Mn_{66}$ and 100% at 935 °C for $Cu_{60}MgAl$. For the other two biomasses, which present lower reactivity, it would be necessary to increase the FR temperature or to use a carbon stripper to obtain CO_2 capture efficiencies over 95%.

Also in the work of Kuang et al.[35] there was an attempt to improve the CLOU effect introducing different materials in CuO-based OCs. The three materials used were iron ore, chrysolite, and limestone. The presence of Fe involves the formation of $CuFe_2O_4$ which has a detrimental effect on the CLOU activity due to the stability of the spinel. On the contrary, the presence of chrysolite and limestone improved the reactivity of the OC, probably due to the catalytic properties of the two materials in char gasification. Moreover, chrysolite seemed to be a better support material for CuO. However, from SEM analysis, it was found that for all the materials their presence inhibited CuO agglomeration at 950 °C.

The interest toward the utilization of waste materials as OCs is increasing. Moldenhauer et al.[53] investigated the performance of ground steel converter slag from the Linz−Donawitz process as an OC in a 10 kW_{th} CLC system. The biomasses used were wood char, wood pellets, and steam-exploded wood pellets (aka black pellets) from Swedish wood. The material showed a developing CLOU activity during the initial hours of operation, and hence, the fuel conversion improved reaching a conversion of CO to CO_2 up to 99.9%. Based on fines production, the particle lifetime was assessed to be 110−170 h.

■ ROLE OF BIOMASS ASH AND THE FATE OF ALKALI

Biomass ashes typically present a high content of alkali, primarily K and Na, which make them highly reactive and which can therefore effectively interact with bed materials in fluidized bed combustors. Albeit, K and Na show a catalytic effect for char gasification,[28,76−80] and this could promote an assisted conversion of biomass, although several alkali-induced negative effects can occur. Their reaction with bed materials could entail the agglomeration of the bed and interfere with normal operation leading eventually to defluidization. Agglomeration is mainly caused by the interaction of alkali with silica, forming low melting points eutectics.[76,79,81−83]

Another critical alkali-induced concern in thermal conversion of biomass is the release of alkali species, during devolatilization and char burnout, in the gas phase.[79,84−86] KCl(g) (gaseous phase) is the predominant released species when Cl is available for reaction; otherwise, KOH(g) dominates, and also K(g) is formed at higher temperatures. The presence of these alkali compounds in the flue gas determines fouling of downstream equipment by condensation of the gaseous species onto the colder surfaces. These deposits reduce the heat transfer coefficient, entail loss of efficiency, and induce severe corrosion.[86,87] The utilization of alternative bed materials in substitution of silica sand may reduce the agglomeration tendency.[88] However, this option results in an increase of alkali concentration in the gas phase. It is clear that this a relevant topic for bio-CLC: Table 2 reports the main studies about the interaction of alkali from biomass ash with OC in CLC. The interest in this topic is witnessed by the fact that many works have been published in the last 2−3 y. Investigations during real CLC tests—in fluidized bed systems—as well as studies about the fate of alkali in the gaseous phase are few, while higher attention was devoted to the interaction between OCs and biomass ash or specific salts used as surrogated ash.

In general, OCs tend to interact with the compounds contained in the biomass ash. The extent of this interaction seems to depend by the nature of both the OCs and the ash compounds and by the operating conditions. The formed compounds can present both positive or negative effects for the OC in terms of reactivity and mechanical properties. About Fe-based OCs, Na-based salts are more reactive with Fe oxides than K-based ones, which entail a reduction of the activity of the OC. Conversely, K−Fe−O compounds are able to increase the reactivity of the OC,[94] at the expense of a simultaneous increment of the agglomeration tendency.[90,94,97]

However, the interaction of potassium compounds with Fe materials is far from straightforward. Gu and co-workers[82] found that SiO_2 plays an important role in the potassium−iron interaction. For K-rich ash, but with a low content of SiO_2 there is an improvement of the reactivity of the OC. Differently, SiO_2-rich ash promotes the formation of molten potassium silicates that lead to an increase of the sintering and of the deactivation of the OC. A similar result was found by Staničić and co-workers[90] where the ternary system formed by K_2CO_3/SiO_2/hematite entailed the formation of new phases with a severe agglomeration tendency, while in the presence of only SiO_2 no interaction occurred.

It is important to underline that the nature of the Fe material is crucial: for example the system K_2CO_3/SiO_2/ilmenite presented a low degree of interaction.[90] In general, ilmenite seems to have less affinity with biomass ash than other Fe oxides. Indeed, ilmenite does not present any interaction with $CaCO_3$, unlike hematite or other iron ores which tend to react with Ca producing calcium ferrites, in particular under reducing environments.[90,94,99] Also tests carried out on LD-slag as OC, a waste material produced in the Linz−Donawitz process, with K_2SO_4 and K_2CO_3 entailed an erichment of K-based compounds in the OC, but without relevant variation in the reactivity.[97]

However, the coexistence of K and P can turn the tables, in particular the presence of KH_2PO_4 seems to have a massive effect on the Fe-based OCs: all authors detected a possible loss of reactivity combined with the occurrence of agglomeration and consequent defluidization.[95,97] Moreover, Zevenhoven and co-workers[95] stated that when defluidization was observed this was caused mainly by KH_2PO_4, while KCl is not expected to give problems in CLC (or oxygen carrier aided combustion (OCAC) conditions), because the temperatures in the system are quite high and most KCl tends to be vaporized.

About the interaction between Mn-based OCs and biomass ash, few works are available in the literature. The results of these latter showed that $CaCO_3$ tends to react with the OC but

https://doi.org/10.1021/acs.energyfuels.1c02600
Energy Fuels 2021, 35, 19248−19265

no evidence of severe agglomeration was detected.[89] Conversely, the effect of K_2CO_3 seemed to depend by the nature of the OC and the reaction environment; specifically, the presence of Si in the OC implied agglomeration problems, and this is in line with the tests carried out on Fe-based OCs and the systems of K_2CO_3/SiO_2, while the presence of Fe seemed to preserve a certain stability. Additionally, MnFeAl OCs did not show as severely agglomerated samples, which is likely due to the Al content.[89] Meanwhile, the presence of Ca determined the formation of $Ca_xMn_yO_z$ compounds.[90] As was also found for the Fe-based OCs, the presence of phosphorus had a heavy effect on the OCs promoting the coating of the particle surface.[89]

The forecasting of these interactions could be crucial in preventing agglomeration, and hence defluidization, with the possible consequence of an abrupt stop of the CLC system. In this case, several authors tried to compare experimental results with thermodynamic predictions.[89,90,94,95] In general, there was a good agreement with Fe-based OCs, but not for Mn-based OCs, and this probably was due to a lack of thermodynamic data for systems including potassium and manganese.

It is worth highlighting that all previously cited works carried out tests using only the OCs and the biomass ash or a surrogated biomass ash, but with the absence of the biomass itself, that means conditions quite far from those really encountered in a CLC system. In their work Cheng and co-workers[93] carried out carbothermal experiments to study the interaction between Fe_2O_3 with different ashes (one from a coal and three from different biomasses) varying the content of biomass carbon. The results showed that in the presence of a high content of biomass carbon no interaction was detected between the OC and the ashes (and no OC reactivity reduction). On the contrary, when the content of biomass carbon was low in the system, reactions between the OC and the ashes occurred with formation of $MgFe_2O_4$, Fe_2SiO_4, and $CaFe_2O_4$ (as schematized in Figure 4), which are more difficult to be reduced than Fe_2O_3.

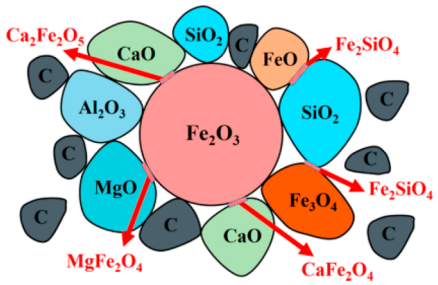

Figure 4. Schematic diagram of the solid-phase reaction between the Fe-based OCs and ash [Reproduced from ref 93. Copyright 2020 American Chemical Society].

Moreover, they suggested that the addition of an appropriate amount of ash to the Fe-based OC can promote the performance of Fe_2O_3. In other words, they indicated that there is an optimum value for the amount of incorporated ash. When this optimum value is exceeded, some foreign ions (K and Na) in the ash interacted with aluminosilicates to form species with low melting points, covering the surface of Fe_2O_3 particles. These findings were also confirmed by the experimental campaigns of Zang[96] and Bhui[98] who detected an improvement of the performance of iron ore and Fe_2O_3 respectively in tests of bio-CLC.

The incomplete understanding of the effect of ash on bio-CLC performance and some discrepancies between tests carried out with only OC-ash systems and under real CLC conditions are also witnessed by the results obtained by Luo et al.[100] in tests carried out cofeeding biomass and coal in a TGA system using CuO as the OC. They observed that the addition of K_2CO_3 and candlenut wood ash reduced the gasification temperature of coal. The co-combustion of biomass and coal improved the reactivity of char due to the presence of alkaline species such as K, Ca, Mn, etc.[101] The XRD analysis indicated negligible interaction between ash and CuO. Also in the work of Gu and co-workers[44] the possible interaction between SiO_2 and Fe_2O_3 was detected under reducing conditions at high temperature, which was not identified by other authors.[90]

Few studies focused on the fate of biomass alkali in the gaseous phase. In particular, Gogolev and co-workers[43,91,92] focused their attention on alkali emissions at the outlet of CLC system both from the FR and the AR. Despite the fact that a lot of work is necessary for a complete comprehension of how several operating condition may influence the release of alkali, some important findings can be summarized. A large amount of alkali was retained in the condensed phase: for example, this retention was recorded to be higher than 97% for ilmenite and higher than 92% for braunite, of which 20−40% was absorbed by the OCs. Indeed, for ilmenite the formation of silicates, aluminosilicates, manganates, and alkali titanates was detected, while for braunite mainly manganates and silicates. However, alkali release can be promoted by steam-rich conditions because the presence of steam accelerates the decomposition of potassium salts with an increased formation and release of KOH(g).[91] Some differences can also be observed on varying the alkali content in the biomass: fuels with high alkali content determined higher emissions form the FR; in particular, the emissions from the FR were several times higher with respect to the AR. On the contrary, in case of low alkali content fuels an amount of emissions from the AR of the same magnitude was recorded, but it was lower than that from the FR.[92] The alkali emissions from the AR are attributable to the combustion of unconverted fuel that is carried over from the FR to the AR as confirmed by the low carbon capture efficiency in the CLC tests.

EFFECT OF VOLATILES ON BIO-CLC

The high content of volatiles in biomass and the fast devolatilization result in a generally ineffective contact between the volatiles and the OC, with a consequent decrease of the CLC system performance, in particular in terms of FR combustion efficiency [The combustion efficiency of the FR represents the ability of the system to convert fuel inside the fuel reactor]. This incomplete conversion of volatiles requires an oxygen polishing step downstream of the FR. To improve the combustion efficiency, the fuel feeding is suggested at the bottom of the FR, as well as the utilization of OCs with a CLOU effect. In addition, the incomplete conversion of volatiles can affect the correct functioning of the downstream equipment due to increased tar formation.

Different authors witnessed the problem related to the slip of volatiles from the bed where the performance of OCs has a critical role. For example, Berdugo Vilches and co-workers[61] experienced unburnt volatiles during bio-CLC tests with ilmenite and manganese ore as OCs and commercial wood pellets as fuel. The accumulated operational time was more than 1000 h in the semicommercial dual fluidized bed (DFB)

https://doi.org/10.1021/acs.energyfuels.1c02600
Energy Fuels 2021, 35, 19248−19265

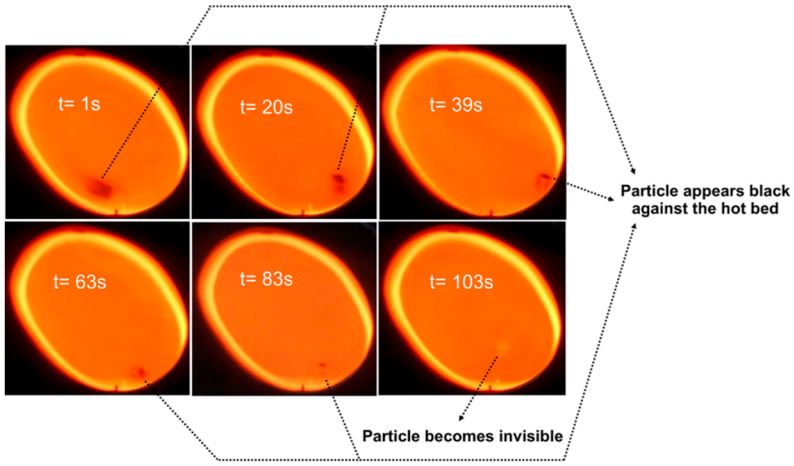

Figure 5. Photographs of a 15 mm wood particle at different residence times during devolatilization under CLC conditions at 875 °C [Reproduced from ref 104. Copyright 2019 American Chemical Society].

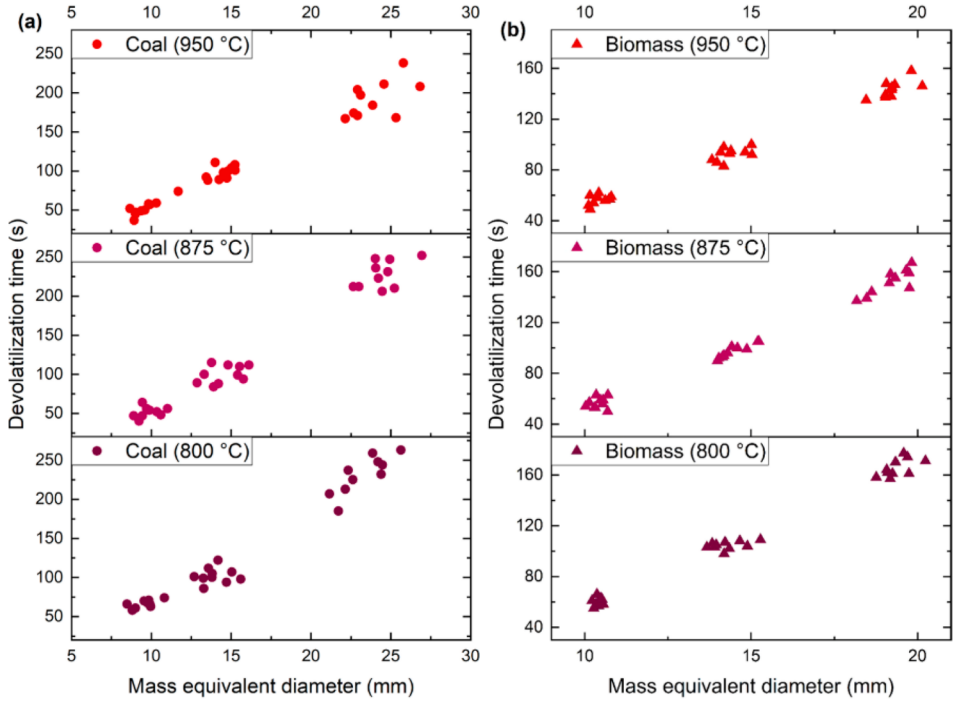

Figure 6. Devolatilization time of (a) coal and (b) biomass for different particle sizes at 800, 875, and 950 °C [Reproduced from ref 104. Copyright 2019 American Chemical Society].

unit at Chalmers University of Technology. In general, they detected CH_4, C_2, and C_3 species at the exit of the FR, which are a clear indication of unconverted volatile products: about 14−16% of the carbon in the fuel ended up as unconverted hydrocarbons including tar. However, increasing the fluidization velocity resulted in a higher combustion efficiency and lower oxygen demand, highlighting the fact that the conversion of gaseous species is limited to a large extent by the effectiveness of the gas−solids mixing. Also, the bed material circulation rate can have a positive effect: a higher circulation rate, as well as a lower fuel feeding rate, tended to improve the volatile conversion within the bed. Under these conditions, the gasification products and volatiles were consumed more rapidly near the char particle, which resulted in an increase of the rate of char gasification. This latter reflects the relationship between the residence time in the FR and the net reactivity of the bed inventory. Insufficient gas−solid mixing can also arise as the biomass particles tend to float to the surface of the bed,[102] thereby releasing a fraction of the volatiles in zones that have a low density of OCs. In addition, fuel particle characteristics have an important role to control, to a certain measure, the amount of unburnt volatiles: for small particles and high volatile contents, carbon slip to AR is almost negligible, but at the expense of lower volatiles conversion.[69]

Pragadeesh and co-workers[103,104] focused their attention on the evaluation of the devolatilization time—both for coal and biomass—under CLC conditions. In particular, they proposed a novel technique, called the "color indistinction method" (CIM), for the determination of the devolatilization time (τ_d) in FB-CLC. The method, as indicated by its name, is based on

https://doi.org/10.1021/acs.energyfuels.1c02600
Energy Fuels 2021, 35, 19248−19265

Table 3. Values of Correlation Parameters for Determining Devolatilization Time of Different Fuels[a]

fuels	A (proportionality constant)	i (size factor)	j (temperature)	k (shape factor)	coefficient of determination, R^2
Indian coal 1	2449	1.489	1.042	0.349	0.959
Indian coal 2	19997	1.39	1.298	0.362	0.956
Indonesian coal	9831	1.666	1.303	0.4	0.966
biomass	293	1.615	0.799	-	0.973
all coals	10421	1.536	1.266	0.376	0.945

[a]Data reprinted with permission from ref 103.

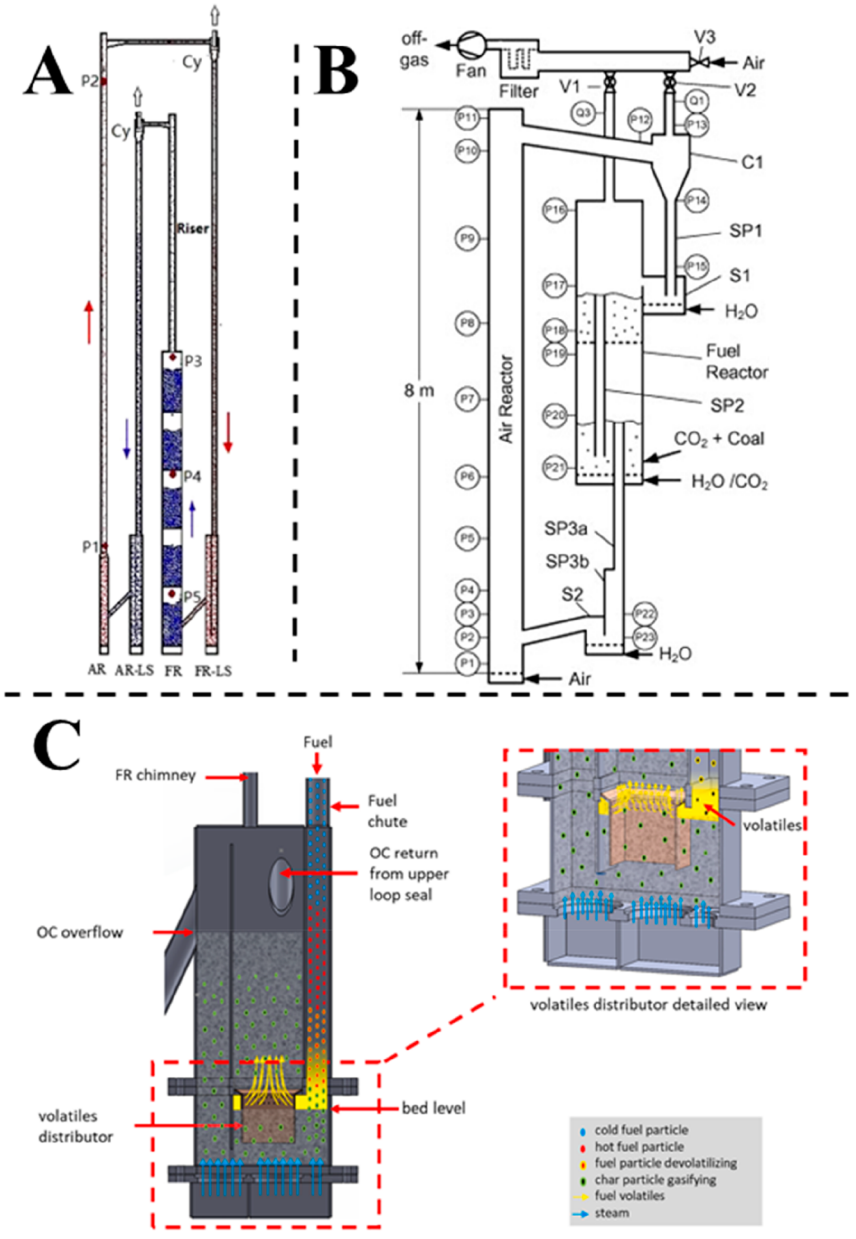

Figure 7. Three different designs proposed for the FR for the improvement of OC−volatiles interaction. (A) Configuration for continuous facility (P1/P2/P3/P4/P5, pressure tapping points; solid arrows, flow direction of the oxygen carrier) [Reproduced from ref 56. Copyright 2018 American Chemical Society]. (B) Schematics of the 25 kWth CLC pilot plant with a two-stage FR at Hamburg University of Technology (S1 and S2: siphon loop seals) [Reprinted with permission from ref 110. Copyright 2013 Elsevier Ltd.]. (C) Fuel reactor and volatiles distributor section view [Reprinted from ref 92].

the color change of the particle surface from black to reddish orange, due to the onset of the char conversion, which occurs just at the end of devolatilization. This change to reddish orange matches the color of the hot bed resulting in the disappearance of the particle. Specifically, the devolatilization time was defined as the time period between the introduction of the fresh fuel particle into the bed and the time of its disappearance (Figure 5). The CIM method successfully

https://doi.org/10.1021/acs.energyfuels.1c02600
Energy Fuels 2021, 35, 19248−19265

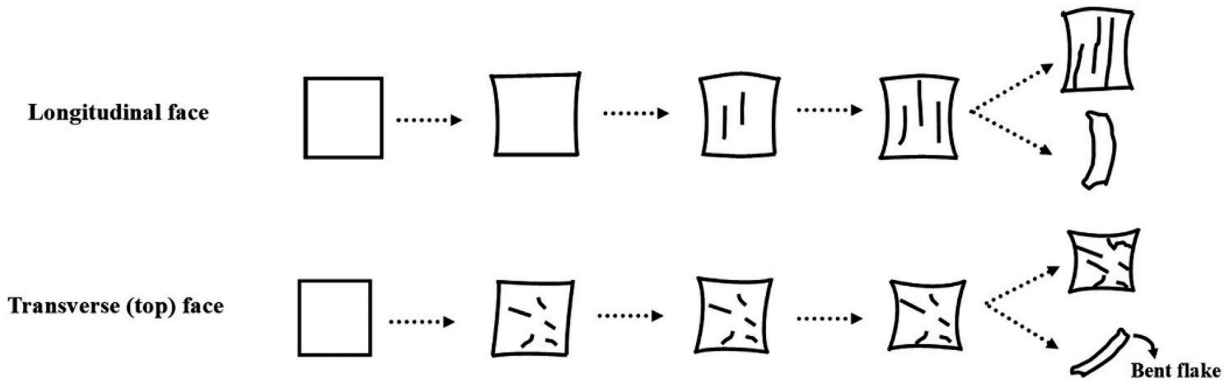

Figure 8. Fragmentation pathway of biomass particles [Reproduced from ref 112. Copyright 2018 American Chemical Society].

determined the devolatilization time of different types of fuel particles, in a range of particle sizes at different bed temperatures (Figure 6), as validated by comparison with other techniques.[104]

With the utilization of above-mentioned technique, they found that the devolatilization time increased with particle size and decreased with the FR temperature, analogous to the behavior observed in conventional fluidized bed combustion. The devolatilization time determined the oxygen carrier demand in the FR, as the release of volatiles is the fastest step during solid fuel conversion. The authors also tried to determine correlations for devolatilization time of fuel particles in CLC conditions, using hematite as OC and three coals and 1 biomass. For conventional combustion, the correlation provided in the literature[105−107] relates devolatilization time as a function of only the particle size. Pragadeesh and co-workers[103] proposed a new correlation that embodies the effects of other parameters such as temperature and particle shape:

$$\tau_d = A d_p^i T^j \varphi^k \quad \text{(R8)}$$

where A is the proportionality constant which takes into account the effects of transient mass and heat transfer within the particles and the devolatilization kinetics,[108] d_p is the particle diameter in millimeters, T is the operating FR temperature, and φ is the sphericity of particles. i,j,k are the empirical exponents of the respective parameters. Particle size is the most influencing parameter for devolatilization followed by the operating FR temperature and sphericity. From the estimation of the different parameters, the parameter A appeared to be the most sensitive with respect to the fuel type (Table 3).

Besides optimized operating conditions (FR temperature, OC recirculation rate/fuel feeding rate, and fluidization velocity) and biomass characteristics (size and shape), several authors tried to limit the amount of unconverted volatiles proposing specific novel designs for the FR.

Jiang et al.[56] proposed a multistaged FR, where four built-in gas distributors divided the reactor into five small sections with the same height, in order to hinder the generation of big bubbles or slugs and for improving the gas−solid contact (Figure 7A). The tests on this configuration were carried out using hematite and sawdust or rice husk as fuel. The results showed that CO could be efficiently converted into CO_2 in the temperature range of 840−900 °C and its conversion was above 90%. Specifically, the FR temperature exhibited positive effects on the fuel conversion and carbon capture efficiency because higher temperatures accelerated the gasification rate and improved the oxygen carrier reactivity. The gas conversion efficiencies were above 90% at temperatures above 840 °C, and no hydrogen was found at the outlet of the FR.

An experimental campaign on a 25 kW_{th} CLC system with a two-staged FR, using lignite and biomass (hardwood pellets) as fuels and CuO supported by Al_2O_3 as OC, was carried out by Haus and co-workers.[109] The FR was divided into two stages[110] (see Figure 7B), FR1 and FR2, by a gas distributor, which was placed between the two beds operated in bubbling mode. The fuel was injected usually into the FR1. The gaseous products, mostly methane (CH_4), hydrogen (H_2), and carbon monoxide (CO), generated in the FR1 rose up into the FR2 together with the fluidization gases and continued the reaction with the oxidized OC entering via S1. Finally, the reduced OC came back into the air reactor via S2. Results confirmed that both fuels (lignite and biomass) benefitted from the two-stage configuration, and the combustible gases were almost completely converted in the second stage. The total oxygen demand was between 1.6 (ground biomass) and 1.7% (ground and sieved biomass) and 1.6% for lignite. Without the second stage, the oxygen demand was 7.5% for the ground biomass, 19.3% for the higher fuel flow of the ground and sieved biomass, and 25.7% for lignite. The difference between the biomasses (ground and ground and sieved) probably is ascribable to the different size of the two fuels. The combustion efficiency reached values in the range of 92−97%, and also the carbon combustion efficiency was high (93−97%). These results demonstrated the effectiveness of this configuration into maximizing the gas−solid contact.

Gogolev and co-workers presented a different solution based on a single stage FR, but with a specific internal configuration.[92] The newly designed FR was part of a 10 kW_{th} CLC system for high volatile conversion tested in an experimental campaign using ilmenite and five biomasses with different volatile and alkali content. The most significant implementation in the reactor design was the addition of a volatiles distributor to the FR internals as shown in Figure 7C. The basic idea, behind the volatiles distributor, is obviously to optimize the contact between volatiles and OC. Since the fluidizing velocity is several times higher than the OC minimum fluidization velocity, the further gas addition due to the volatile release would tend to pass though the bed as large bubbles, limiting the volatile-solid contact. The volatiles distributor is composed by a perforated internal baffle, which hinders the formation of big bubbles and divides the volatiles

https://doi.org/10.1021/acs.energyfuels.1c02600
Energy Fuels 2021, 35, 19248−19265

Table 4. Tar Composition for the CLOU Tests with Three Types of Biomass[a]

biomass	pine sawdust			olive stone			almond shell		
				Temperatures (°C)					
fuel reactor	775	800	825	775	800	825	775	800	825
air reactor	800	800	800	800	800	800	800	800	800
				Tar Composition (g/Nm^3 dry)					
benzene, 1 propenyl	[b]	1×10^{-4}	[b]	1.7×10^{-3}	[b]	1.9×10^{-3}	1×10^{-4}	[b]	5×10^{-4}
dodecane	4×10^{-4}	1×10^{-3}	6×10^{-3}	1.8×10^{-3}	[b]	[b]	9×10^{-4}	2×10^{-4}	7×10^{-4}
indene	[b]	[b]	[b]	6×10^{-4}	1.1×10^{-3}	1.4×10^{-3}	[b]	[b]	3×10^{-4}
tetradecane	4×10^{-4}	5×10^{-4}	3.2×10^{-3}	[b]	[b]	[b]	7×10^{-4}	2×10^{-4}	5×10^{-4}
naphthalene	2×10^{-4}	3×10^{-4}	7×10^{-4}	10.5×10^{-3}	19.4×10^{-3}	11.9×10^{-3}	1×10^{-4}	0.0000	1.7×10^{-3}
2,6,10 trimethyltridecane	2×10^{-4}	3×10^{-4}	2.5×10^{-3}	[b]	[b]	[b]	5×10^{-4}	1×10^{-4}	[b]
naphthalene 2-methyl	[b]	[b]	[b]	1.1×10^{-3}	1.6×10^{-3}	1.6×10^{-3}	[b]	[b]	[b]
naphthalene 1-methyl	[b]	[b]	[b]	7×10^{-4}	1.1×10^{-3}	1.1×10^{-3}	[b]	[b]	[b]
biphenil	[b]	[b]	[b]	9×10^{-4}	1.4×10^{-3}	1.0×10^{-3}	[b]	[b]	[b]
benzophenone	[b]	[b]	[b]	[b]	[b]	[b]	4×10^{-4}	[b]	[b]
acenaphthylene	0.0000	[b]	[b]	4×10^{-4}	[b]	9×10^{-4}	[b]	[b]	[b]
fluoranthene	[b]	[b]	[b]	[b]	[b]	[b]	[b]	[b]	[b]
phenantrene	[b]	[b]	9×10^{-4}	1.4×10^{-3}	[b]	[b]	[b]	[b]	[b]
total tar (g/Nm^3 dry)	0.001	0.002	0.013	0.019	0.025	0.020	0.003	0.001	0.004

[a]Data reprinted with permission from ref 116. [b]The compound was not identified.

flow into multiple streams, thus increasing contact with the OC. The system demonstrated its efficiency obtaining a carbon capture efficiency close to 100% for typical biomass fuels with high content of volatiles and higher than 94% for low volatiles fuels.

Another consequence of the high volatile content of biomass is the occurrence of primary fragmentation during the devolatilization stage.[111] Primary fragmentation affects the rate of fuel conversion, emissions, and fine particulates generation in an FR, thus constituting a critical design input. Two specific works were focused on the investigation of the char conversion rate and the attrition of various fuel particles under fluidized bed CLC conditions.[112,113] Fragmentation of fuel particles immediately after the introduction into a combustion environment was attributed to the thermal shock created by the temperature gradient, which often results in a large number of fragments. During the later stages of devolatilization, fragmentation occurred due to the mechanical stresses created by the evolution of volatile matter at high temperatures. Specifically for biomass, these authors proposed a pathway for particle fragmentation, which individuated the development of cracks until the final stages of devolatilization with simultaneous shrinkage. Just before the end of devolatilization, the particles started to fail at places where the stresses created by shrinkage superseded the particle strength, along the crack line (Figure 8); the fragments were usually bent flakes which defoliated from the surface. The number of fragments was found to be high for large particles and also at higher temperatures.

As regards tar formation in CLC systems, the literature is rather poor: Zheng et al.[114] and Boot-Handford et al.[115] investigated the effectiveness of some OCs for the conversion of volatile matter. Fe_2O_3 (pure), Fe_2O_3 (on alumina), CuO (on mayenite), and Cu_2O (on mayenite) were used as OCs. Both works found that tar was mostly combusted to CO_2. Zheng et al. found that mayenite-supported CuO was the most reactive with the pyrolysis products and was particularly effective for converting tar and char at 1173 K, due to its CLOU effect. Boot-Handford et al. documented carbon deposition on Fe_2O_3 which was removed during the oxidation stage without any significant effects on the reactivity of the OCs. These results confirm that the main problem of unconverted volatiles is related to the poor contact between OC and gaseous products.

Pérez-Astray et al.[116] monitored tar formation during the operation of a 1.5 kW_{th} CLC apparatus consisting of two interconnected fluidized bed reactors. The tests were carried out under two different modes: under CLOU mode using a Cu−Mn mixed oxide (named as $Cu_{34}Mn_{66}$-GR) and under iG-CLC mode using a Fe-based ore (hematite). Three biomass wastes were used as fuels: pine sawdust, olive stone, and almond shell. The results showed that the total tar ranged between 2.5 and 3.7 g/Nm^3 under iG-CLC mode at the highest temperature, mostly consisting of naphthalene. This makes necessary a further oxygen polishing step to condition the stream for subsequent transport and storage or utilization. Under CLOU mode, lower amounts of tar were found (Table 4), although in this case also linear or branched hydrocarbons were detected.

In the same paper, Pérez-Astray et al. also investigated the fate of fuel-N by monitoring the formation of NOx. The findings revealed that fuel-N conversion improved under iG-CLC mode. However, in both modes the fuel-N appeared as N_2 at the FR outlet with only little presence of NO for all temperatures investigated. The only difference lied in the relation between N_2 and NOx emitted which was higher in the case of iG-CLC due to the absence of free oxygen that favors NO formation. Some differences in the amount of formed NO were detected between biomasses under CLOU mode and were attributed to the different char reactivity of the three types of biomasses. Little amounts of N_2O were detected under CLOU mode, and only at temperatures lower than 850 °C. Finally, at the outlet of the AR—under both combustion modes—NO was detected but its concentration decreased when the FR temperature increased. However, these values never exceeded the current limits for power plants.

https://doi.org/10.1021/acs.energyfuels.1c02600
Energy Fuels 2021, 35, 19248−19265

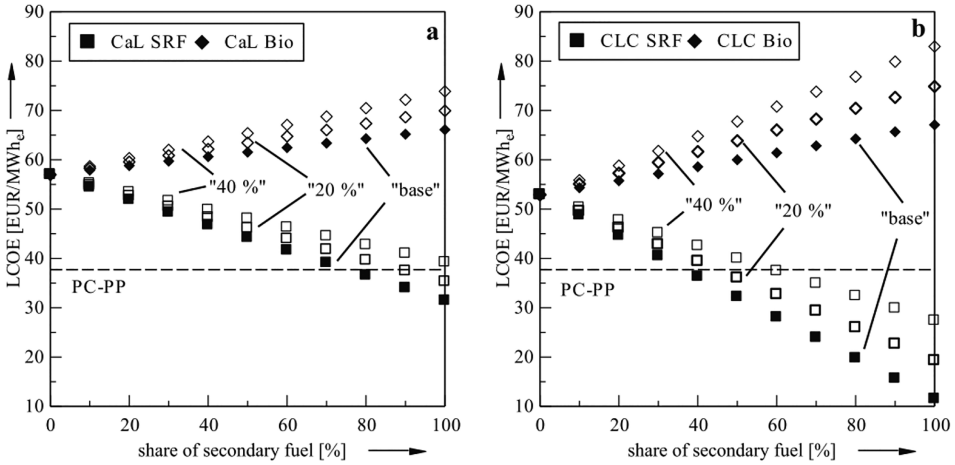

Figure 9. LCOE of the CaL case (a) and CLC case (b) depending on the share of secondary fuel and economic scenario. The "base" economic scenario refers to boundary conditions of a coal-fired unit, whereas "20%" and "40%" represent an increase in investment and maintenance cost by 20 or 40% for the corresponding share of secondary fuel, respectively [Reprinted with permission from ref 131. Copyright 2019 Springer Nature B.V.].

BIO-CLC MODELING: PERFORMANCE EVALUATION, SYSTEM INTEGRATION, AND TECHNO-ECONOMIC ANALYSIS

In general, process modeling is a good tool to forecast system performance, to optimize operating conditions, and to create detailed design, avoiding useful but time-consuming and often expensive experimental campaigns. This is also true for bio-CLC. Several works, not many, can be found in the literature which mainly focus on the performance simulation of bio-CLC systems.[117−121] All these works present a good match with the experimental data.

Noteworthy, the work of Abad and co-workers[122] is quite interesting because it proposed a simple model to facilitate the comparison of the performance of different OC−solid fuel pairs in an iG-CLC system. The model was based on the utilization of the kinetic parameters for char gasification and the reaction between the OC and the combustion gases to calculate the CO_2 capture efficiency and the total oxygen demand as parameters for comparison purposes. The model was validated using two Fe-based OCs (ilmenite and Tierga ore) in pairs with five different fuels: one anthracite, one sub-bituminous coal, two bituminous coals, and one biomass (olive tree pruning). The model was able to replicate some of the main results previously reported in the literature, confirming that, for a good evaluation of the potential of an oxygen carrier−solid fuel pair, the most influencing variables are the FR temperature and the solids circulation rate between the FR and AR.

Other authors evaluated the performance of integrated systems consisting of bio-CLC and power generation systems or CO_2 utilization processes. The performance of a combined system of bio-CLC and an organic Rankine cycle were studied by two different research groups.[123,124] Both works evaluated a net energy efficiency of about 19% that is higher than the average electrical efficiency of small-scale biomass-based CHP (17%) reported by Intelligent Energy Europe.[125] Moreover, the overall thermal efficiency was reported to reach 21% at 30 MPa for a bio-CLC/supercritical CO_2 Brayton cycle system for power generation.[126] Integration of bio-CLC with steam turbine CHP plants evidenced that this configuration presents a very small net efficiency penalty (less than 1% point) in comparison to the reference plant with a conventional boiler operating at the same fuel input and the same heat production. In the works of Bareschino et al.[127] and Mancusi et al.[128] the integration of bio-CLC—for CO_2 production—with an electrolyzer—for H_2 production—was investigated for the production of methane and methanol by CO_2 hydrogenation. The results showed that the electric energy conversion efficiency for methanol production was about 30%, and this value was higher than that evaluated for methane production, suggesting that methanol production could be more effective than methane production with respect to the electric energy storage efficiency.

Different authors proposed several techno-economic analyses (TEAs) related to bio-CLC. Lindroos at al.[129] focused the investigation to some critical parameters for the development of bio-CLC. Their analysis, developed in an EU contest [Application of the Emission Trading System (ETS)], highlighted that the bio-CLC process is a robust investment if the net-income from the captured bio-CO_2 is about 10 €/tCO_2 or higher; otherwise, the technology works badly. Moreover, other critical parameters raised by the authors are a biomass price higher than 30 €/MWh or a selling electricity price lower than 30 €/MWh. The biomass price-related issue was also individuated by Keller et al.[130] in the Japanese scenario, together with the high cost of transporting liquefied CO_2. Haaf and co-workers[131] compared the economic performances of a CLC system with a calcium looping (CaL) system which retrofits an existing pulverized coal power plant (PC-PP). In particular, they evaluated the impact of the type of fuel used for feeding the FR and the calciner for CLC and CaL, respectively. The fuels fed to the FR and calciner were fuel blends consisting of two different types of fuel [hard coal + biomass, hard coal + solid recovered fuel (SRF)]. The share between hard coal and biomass/SRF was varied to understand their impact on the economic performance. The results of TEA showed that the differences between CaL and CLC for 100% hard coal firing were negligible in terms of levelized cost of energy (LCOE) (CaL 56.97 EUR/MWh$_e$ vs CLC 52.90 EUR/MWh$_e$). The LCOE increased along with a higher share of biomass cofiring both for the CaL

https://doi.org/10.1021/acs.energyfuels.1c02600
Energy Fuels 2021, 35, 19248−19265

and CLC scenarios (Figure 9); for SRF, the trend was opposite. Again, the cost of biomass resulted as a crucial point for CLC. The LCOE of CaL matched that of power generation without CCS at a share of about 80% of SRF in the feeding fuel for the calciner. For CLC, this value was approximately 50% of SRF.

CONCLUSIONS AND FUTURE RESEARCH PERSPECTIVES

After more than two decades of research, chemical looping combustion appears to be a rather mature technology, which will be presumably ready for commercialization in the next few years. The main technical challenges for CLC scale-up have already been identified:[13] adequate control of circulation, suitable low-cost, reactive and attrition-resistant OCs, and downstream polishing treatment. When it comes to the combustion of biomass in CLC, some additional challenges have been reported, which need to be adequately taken into consideration. In detail,

(1) Cheap OCs, like natural ores or waste residues, will be most likely the only reasonable choice for bio-CLC. Structural modifications, deactivation by alkali or by other ash related compounds, attrition, all make the use of expensive synthetic OCs prohibitive. Future research should be focused to find the best compromise between price, oxygen carrying capacity, reactivity, mechanical resistance, and resistance to deactivation. This would probably imply considering in detail the ash composition of the biomass to be used in the process.

(2) OCs with even partial CLOU properties have a distinct advantage over all other OCs when converting solid fuels. While this aspect is crucial with coal or other fossil fuels, operational experience has demonstrated better conversion also with biomass. Using natural ores or waste residues with CLOU properties appears to be a promising strategy to optimize the performance of bio-CLC.

(3) The biomass ash components, and especially alkali, do interact extensively with the OC bed material. While some general trends are often found (increase of reactivity and of agglomeration tendency), some exceptions have been reported. With this respect the composition of the ash and of the OC appears to be crucial, especially the presence of silica and phosphorus. More research on this topic is absolutely necessary, as well as on the occurrence of volatile alkali in the gaseous outlet streams.

(4) Bypass of the volatile matter generated from biomass pyrolysis with respect to the OC bed is probably the most challenging problem to be solved. Incomplete carbon conversion, tar formation, the need of a downstream polishing step, all result from this issue. More studies are necessary for developing very reactive OCs and also to understand the role of the biomass nature, in terms of composition, on the process. While partial recycling of the outlet gaseous stream and optimization of the operating conditions may be beneficial, acting on the design, and hence on the fluid-dynamics, of the FR appears to be the most promising approach. The few attempts on this path have provided encouraging results, so that this research topic should be more extensively exploited in the future.

(5) Up to now quite few works have been carried out on bio-CLC modeling, either for performance evaluation, for system integration, or for techno-economic analysis. Some promising results have been reported, which however need to be confirmed by more extensive work, also taking into account the relevant key aspects for scale-up. Bio-CLC has enormous potential which has been explored in a rather limited way so far.

AUTHOR INFORMATION

Corresponding Author

Fabrizio Scala − *STEMS, Consiglio Nazionale delle Ricerche, 80125 Napoli, Italy; DICMaPI, Università degli Studi di Napoli Federico II, 80125 Napoli, Italy;* orcid.org/0000-0003-1239-453X; Email: fabrizio.scala@unina.it

Author

Antonio Coppola − *STEMS, Consiglio Nazionale delle Ricerche, 80125 Napoli, Italy*

Complete contact information is available at: https://pubs.acs.org/10.1021/acs.energyfuels.1c02600

Notes

The authors declare no competing financial interest.

Biographies

Antonio Coppola graduated from the University of Naples Federico II in 2009, where he got his Ph.D. in 2013. He was a research fellow at IRC-CNR from 2014 until 2018 and at the University Federico II from 2018 until 2019. Since 2019 he has been a researcher at STEMS-CNR. His activities are related to thermal valorization of biomasses in FB reactors, carbon capture, utilization, and storage (CCUS), and techno-economic analysis. He is the author of more than 100 publications in journals and conference proceedings.

Fabrizio Scala graduated from the University of Naples Federico II in 1995, where he got Ph.D. in 1999. He was a researcher at IRC-CNR from 2001 until 2014, when he became an associate professor at the University Federico II. Since 2020 he has been a full professor. His activities are related to combustion, gasification, and pyrolysis in FB reactors, and carbon capture, utilization, and storage (CCUS). He is the author of more than 200 publications in journals, volumes, books, and conference proceedings.

REFERENCES

(1) Lyngfelt, A.; Leckner, B.; Mattisson, T. A Fluidized-Bed Combustion Process with Inherent CO2 Separation; Application of Chemical-Looping Combustion. *Chem. Eng. Sci.* **2001**, *56* (10), 3101−3113.

(2) Lewis, W. K.; Gilliland, E. R. Production of Pure Carbon Dioxide. US Patent US2665972A, January 12, 1954.

(3) Richter, H. J.; Knoche, K. F. Reversibility of Combustion Processes. *ACS Symp. Ser.* **1983**, *235*, 71.

(4) Ishida, M.; Zheng, D.; Akehata, T. Evaluation of a Chemical-Looping-Combustion Power-Generation System by Graphic Exergy Analysis. *Energy* **1987**, *12* (2), 147−154.

(5) Ishida, M.; Jin, H. A New Advanced Power-Generation System Using Chemical-Looping Combustion. *Energy* **1994**, *19* (4), 415−422.

(6) Ishida, M.; Jin, H. A Novel Combustor Based on Chemical-Looping Reactions and Its Reaction Kinetics. *J. Chem. Eng. Jpn.* **1994**, *27* (3), 296−301.

(7) Farooqui, A.; Bose, A.; Ferrero, D.; Llorca, J.; Santarelli, M. Techno-Economic and Exergetic Assessment of an Oxy-Fuel Power

Plant Fueled by Syngas Produced by Chemical Looping CO2 and H2O Dissociation. *J. CO2 Util.* **2018**, *27* (September), 500−517.
(8) Shijaz, H.; Attada, Y.; Patnaikuni, V. S.; Vooradi, R.; Anne, S. B. Analysis of Integrated Gasification Combined Cycle Power Plant Incorporating Chemical Looping Combustion for Environment-Friendly Utilization of Indian Coal. *Energy Convers. Manage.* **2017**, *151* (September), 414−425.
(9) Zhu, L.; Jiang, P.; Fan, J. Comparison of Carbon Capture IGCC with Chemical-Looping Combustion and with Calcium-Looping Process Driven by Coal for Power Generation. *Chem. Eng. Res. Des.* **2015**, *104*, 110−124.
(10) Jiménez Álvaro, Á.; López Paniagua, I.; González Fernández, C.; Rodríguez Martín, J.; Nieto Carlier, R. Simulation of an Integrated Gasification Combined Cycle with Chemical-Looping Combustion and Carbon Dioxide Sequestration. *Energy Convers. Manage.* **2015**, *104*, 170−179.
(11) Lyngfelt, A.; Thunman, H.; Thomas, D. C. B. T.-C. D. C.; S, D. G. F. Chapter 36−Construction and 100 h of Operational Experience of A 10-KW Chemical-Looping Combustor. *Carbon Dioxide Capture for Storage in Deep Geologic Formations* **2005**, 625−645.
(12) Lyngfelt, A.; Brink, A.; Langørgen, Ø.; Mattisson, T.; Rydén, M.; Linderholm, C. 11,000h of Chemical-Looping Combustion Operation—Where Are We and Where Do We Want to Go? *Int. J. Greenhouse Gas Control* **2019**, *88* (June), 38−56.
(13) Lyngfelt, A. Chemical Looping Combustion: Status and Development Challenges. *Energy Fuels* **2020**, *34* (8), 9077−9093.
(14) Abanades, J. C.; Arias, B.; Lyngfelt, A.; Mattisson, T.; Wiley, D. E.; Li, H.; Ho, M. T.; Mangano, E.; Brandani, S. Emerging CO2 Capture Systems. *Int. J. Greenhouse Gas Control* **2015**, *40*, 126−166.
(15) Abuelgasim, S.; Wang, W.; Abdalazeez, A. A Brief Review for Chemical Looping Combustion as a Promising CO2 Capture Technology: Fundamentals and Progress. *Sci. Total Environ.* **2021**, *764*, 142892.
(16) Mattisson, T.; Keller, M.; Linderholm, C.; Moldenhauer, P.; Rydén, M.; Leion, H.; Lyngfelt, A. Chemical-Looping Technologies Using Circulating Fluidized Bed Systems: Status of Development. *Fuel Process. Technol.* **2018**, *172* (October 2017), 1−12.
(17) Mattisson, T.; Lyngfelt, A.; Leion, H. *Int. J. Greenhouse Gas Control* **2009**, *3*, 11−19.
(18) Abad, A.; Cuadrat, A.; Mendiara, T.; García-Labiano, F.; Gayán, P.; De Diego, L. F.; Adánez, J. Low-Cost Fe-Based Oxygen Carrier Materials for the IG-CLC Process with Coal. 2. *Ind. Eng. Chem. Res.* **2012**, *51* (50), 16230−16241.
(19) Wang, Y.; Tian, X.; Zhao, H.; Liu, K. The Use of a Low-Cost Oxygen Carrier Prepared from Red Mud and Copper Ore for in Situ Gasification Chemical Looping Combustion of Coal. *Fuel Process. Technol.* **2020**, *205* (December2019), 106460.
(20) Matzen, M.; Pinkerton, J.; Wang, X.; Demirel, Y. Use of Natural Ores as Oxygen Carriers in Chemical Looping Combustion: A Review. *Int. J. Greenhouse Gas Control* **2017**, *65* (August), 1−14.
(21) Pachauri, R. K.; Allen, M. R.; Barros, V. R.; Broome, J.; Cramer, W.; Christ, R.; Church, J. A.; Clarke, L.; Dahe, Q.; Dasgupta, P. *Climate Change 2014: Synthesis Report. Contribution of Working Groups I, II and III to the Fifth Assessment Report of the Intergovernmental Panel on Climate Change*; IPCC, 2014.
(22) Kemper, J. Biomass and Carbon Dioxide Capture and Storage: A Review. *Int. J. Greenhouse Gas Control* **2015**, *40*, 401−430.
(23) Fuss, S.; Canadell, J. G.; Peters, G. P.; Tavoni, M.; Andrew, R. M.; Ciais, P.; Jackson, R. B.; Jones, C. D.; Kraxner, F.; Nakicenovic, N.; Le Quéré, C.; Raupach, M. R.; Sharifi, A.; Smith, P.; Yamagata, Y. Betting on Negative Emissions. *Nat. Clim. Change* **2014**, *4* (10), 850−853.
(24) Pröll, T.; Zerobin, F. Biomass-Based Negative Emission Technology Options with Combined Heat and Power Generation. *Mitig. Adapt. Strateg. Glob. Chang.* **2019**, *24* (7), 1307−1324.
(25) Lyngfelt, A.; Linderholm, C. Chemical-Looping Combustion of Solid Fuels - Status and Recent Progress. *Energy Procedia* **2017**, *114* (November), 371−386.
(26) Lyngfelt, A. *Appl. Energy* **2014**, *113*, 1869−1873.
(27) Jenkins, B.M; Baxter, L.L; Miles, T.R; Miles, T.R Combustion Properties of Biomass. *Fuel Process. Technol.* **1998**, *54* (1−3), 17−46.
(28) Mims, C. A.; Pabst, J. K. Alkali-Catalyzed Carbon Gasification Kinetics: Unification of H2O, D2O, and CO2 Reactivities. *J. Catal.* **1987**, *107* (1), 209−220.
(29) Keller, M.; Arjmand, M.; Leion, H.; Mattisson, T. Interaction of Mineral Matter of Coal with Oxygen Carriers in Chemical-Looping Combustion (CLC). *Chem. Eng. Res. Des.* **2014**, *92* (9), 1753−1770.
(30) Wu, J.; Shen, L.; Xiao, J.; Wang, L.; Hao, J. Chemical Looping Combustion of Sawdust in a 10 KWth Interconnected Fluidized Bed. *J. Chem. Ind. Eng. Soc. China* **2009**, 8.
(31) Huijun, G.; Laihong, S.; Fei, F.; Shouxi, J. Experiments on Biomass Gasification Using Chemical Looping with Nickel-Based Oxygen Carrier in a 25 KWth Reactor. *Appl. Therm. Eng.* **2015**, *85*, 52−60.
(32) Adánez-Rubio, I.; Pérez-Astray, A.; Mendiara, T.; Izquierdo, M. T.; Abad, A.; Gayán, P.; de Diego, L. F.; García-Labiano, F.; Adánez, J. Chemical Looping Combustion of Biomass: CLOU Experiments with a Cu-Mn Mixed Oxide. *Fuel Process. Technol.* **2018**, *172* (September), 179−186.
(33) Haus, J.; Feng, Y.; Hartge, E.-U.; Heinrich, S.; Werther, J. High Volatiles Conversion in a Dual Stage Fuel Reactor System for Chemical Looping Combustion of Wood Biomass. In *International Conference on Negative CO2 Emissions*, 2018.
(34) Adánez-Rubio, I.; Pérez-Astray, A.; Abad, A.; Gayán, P.; De Diego, L. F.; Adánez, J. Chemical Looping with Oxygen Uncoupling: An Advanced Biomass Combustion Technology to Avoid CO2 Emissions. *Mitig. Adapt. Strateg. Glob. Chang.* **2019**, *24* (7), 1293−1306.
(35) Kuang, C.; Wang, S.; Luo, M.; Cai, J.; Zhao, J. Investigation of CuO-Based Oxygen Carriers Modified by Three Different Ores in Chemical Looping Combustion with Solid Fuels. *Renewable Energy* **2020**, *154*, 937−948.
(36) Shen, L.; Wu, J.; Xiao, J.; Song, Q.; Xiao, R. Chemical-Looping Combustion of Biomass in a 10 KWth Reactor with Iron Oxide as an Oxygen Carrier. *Energy Fuels* **2009**, *23* (5), 2498−2505.
(37) Huseyin, S.; Wei, G. Q.; Li, H. B.; He, F.; Huang, Z. Chemical-Looping Gasification of Biomass in a 10 KWth Interconnected Fluidized Bed Reactor Using Fe2O3/Al2O3 Oxygen Carrier. *Ranliao Huaxue Xuebao/Journal Fuel Chem. Technol.* **2014**, *42* (8), 922−931.
(38) Wei, G.; He, F.; Huang, Z.; Zheng, A.; Zhao, K.; Li, H. Continuous Operation of a 10 KWth Chemical Looping Integrated Fluidized Bed Reactor for Gasifying Biomass Using an Iron-Based Oxygen Carrier. *Energy Fuels* **2015**, *29* (1), 233−241.
(39) Wei, G.; He, F.; Zhao, Z.; Huang, Z.; Zheng, A.; Zhao, K.; Li, H. Performance of Fe-Ni Bimetallic Oxygen Carriers for Chemical Looping Gasification of Biomass in a 10 KWth Interconnected Circulating Fluidized Bed Reactor. *Int. J. Hydrogen Energy* **2015**, *40* (46), 16021−16032.
(40) Schmitz, M.; Linderholm, C.; Lyngfelt, A. Chemical Looping Combustion of Sulphurous Solid Fuels Using Spray-Dried Calcium Manganate Particles as Oxygen Carrier. *Energy Procedia* **2014**, *63*, 140−152.
(41) Schmitz, M.; Linderholm, C. J. Performance of Calcium Manganate as Oxygen Carrier in Chemical Looping Combustion of Biochar in a 10 KW Pilot. *Appl. Energy* **2016**, *169*, 729−737.
(42) Schmitz, M.; Linderholm, C. J.; Lyngfelt, A. Chemical Looping Combustion of Four Different Solid Fuels Using a Manganese-Silicon-Titanium Oxygen Carrier. *Int. J. Greenhouse Gas Control* **2018**, *70* (July), 88−96.
(43) Gogolev, I.; Linderholm, C.; Gall, D.; Schmitz, M.; Mattisson, T.; Pettersson, J. B. C.; Lyngfelt, A. Chemical-Looping Combustion in a 100kW Unit Using a Mixture of Synthetic and Natural Oxygen Carriers − Operational Results and Fate of Biomass Fuel Alkali. *Int. J. Greenhouse Gas Control* **2019**, *88* (February), 371−382.
(44) Gu, H.; Shen, L.; Xiao, J.; Zhang, S.; Song, T. Chemical Looping Combustion of Biomass/Coal with Natural Iron Ore as Oxygen Carrier in a Continuous Reactor. *Energy Fuels* **2011**, *25* (1), 446−455.

https://doi.org/10.1021/acs.energyfuels.1c02600
Energy Fuels 2021, 35, 19248−19265

(45) Niu, X.; Shen, L.; Gu, H.; Jiang, S.; Xiao, J. Characteristics of Hematite and Fly Ash during Chemical Looping Combustion of Sewage Sludge. *Chem. Eng. J.* **2015**, *268*, 236−244.
(46) Mendiara, T.; Abad, A.; de Diego, L. F.; García-Labiano, F.; Gayán, P.; Adánez, J. Biomass Combustion in a CLC System Using an Iron Ore as an Oxygen Carrier. *Int. J. Greenhouse Gas Control* **2013**, *19*, 322−330.
(47) Mendiara, T.; Gayán, P.; García-Labiano, F.; De Diego, L. F.; Pérez-Astray, A.; Izquierdo, M. T.; Abad, A.; Adánez, J. Chemical Looping Combustion of Biomass: An Approach to BECCS. *Energy Procedia* **2017**, *114* (November), 6021−6029.
(48) Mendiara, T.; Pérez-Astray, A.; Izquierdo, M. T.; Abad, A.; de Diego, L. F.; García-Labiano, F.; Gayán, P.; Adánez, J. Chemical Looping Combustion of Different Types of Biomass in a 0.5 KWth Unit. *Fuel* **2018**, *211* (October), 868−875.
(49) Linderholm, C.; Schmitz, M. Chemical-Looping Combustion of Solid Fuels in a 100 KW Dual Circulating Fluidized Bed System Using Iron Ore as Oxygen Carrier. *J. Environ. Chem. Eng.* **2016**, *4* (1), 1029−1039.
(50) Ge, H.; Guo, W.; Shen, L.; Song, T.; Xiao, J. Biomass Gasification Using Chemical Looping in a 25kWth Reactor with Natural Hematite as Oxygen Carrier. *Chem. Eng. J.* **2016**, *286*, 174−183.
(51) Abad, A.; Pérez-Vega, R.; Pérez-Astray, A.; Mendiara, T.; de Diego, L.; Garcá-Labiano, F.; Adánez, J. Biomass Combustion with CO2 Capture by Chemical Looping: Experimental Results in a 50 KWth Pilot Plant. In *International Conference on Negative CO2 Emissions*, 2018.
(52) Moldenhauer, P.; Linderholm, C.; Rydén, M.; Lyngfelt, A. Experimental Investigation of Chemical-Looping Combustion and Chemical-Looping Gasification of Biomass-Based Fuels Using Steel Converter Slag as Oxygen Carrier. In *International Conference on Negative CO2 Emissions*, Gothenburg, Sweden, 2018.
(53) Moldenhauer, P.; Linderholm, C.; Rydén, M.; Lyngfelt, A. Avoiding CO2 Capture Effort and Cost for Negative CO2 Emissions Using Industrial Waste in Chemical-Looping Combustion/Gasification of Biomass. *Mitig. Adapt. Strateg. Glob. Chang.* **2020**, *25* (1), 1−24.
(54) Ohlemüller, P.; Ströhle, J.; Epple, B. Chemical Looping Combustion of Hard Coal and Torrefied Biomass in a 1 MWth Pilot Plant. *Int. J. Greenhouse Gas Control* **2017**, *65* (August), 149−159.
(55) Yan, J.; Shen, L.; Jiang, S.; Wu, J.; Shen, T.; Song, T. Combustion Performance of Sewage Sludge in a Novel CLC System with a Two-Stage Fuel Reactor. *Energy Fuels* **2017**, *31* (11), 12570−12581.
(56) Jiang, S.; Shen, L.; Yan, J.; Ge, H.; Song, T. Performance in Coupled Fluidized Beds for Chemical Looping Combustion of CO and Biomass Using Hematite as an Oxygen Carrier. *Energy Fuels* **2018**, *32* (12), 12721−12729.
(57) Linderholm, C.; Knutsson, P.; Schmitz, M.; Markström, P.; Lyngfelt, A. Material Balances of Carbon, Sulfur, Nitrogen and Ilmenite in a 100kW CLC Reactor System. *Int. J. Greenhouse Gas Control* **2014**, *27*, 188−202.
(58) Linderholm, C.; Schmitz, M.; Knutsson, P.; Källén, M.; Lyngfelt, A. Use of Low-Volatile Solid Fuels in a 100 KW Chemical-Looping Combustor. *Energy Fuels* **2014**, *28* (9), 5942−5952.
(59) Linderholm, C.; Schmitz, M.; Knutsson, P.; Lyngfelt, A. Chemical-Looping Combustion in a 100-KW Unit Using a Mixture of Ilmenite and Manganese Ore as Oxygen Carrier. *Fuel* **2016**, *166*, 533−542.
(60) Haus, J.; Hartge, E. U.; Werther, J.; Heinrich, S. Effects of a Two-Stage Fuel Reactor on Chemical Looping Combustion with Methane, Bituminous Coal, Lignite and Wood Biomass. In *5th International Conference on Chemical Looping*, 2018.
(61) Berdugo Vilches, T.; Lind, F.; Rydén, M.; Thunman, H. Experience of More than 1000 h of Operation with Oxygen Carriers and Solid Biomass at Large Scale. *Appl. Energy* **2017**, *190*, 1174−1183.
(62) Pikkarainen, T.; Hiltunen, I.; Teir, S. Piloting of Bio-CLC for BECCS. In *4th International Conference on Chemical Looping*, 2016.
(63) Langørgen, Ø.; Saanum, I. Chemical Looping Combustion of Wood Pellets in a 150 KWth CLC Reactor. In *International Conference on Negative CO2 Emissions*, 2018.
(64) Penthor, S.; Fuchs, J.; Benedikt, F.; Schmid, J. C.; Mauerhofer, A. M.; Mayer, K.; Hofbauer, H. First Results from an 80 KW Dual Fluidized Bed Pilot Unit for Solid Fuels at TU Wien. In *5th International Conference on Chemical Looping*, 2018.
(65) Knutsson, P.; Linderholm, C. Characterization of Ilmenite Used as Oxygen Carrier in a 100 KW Chemical-Looping Combustor for Solid Fuels. *Appl. Energy* **2015**, *157*, 368−373.
(66) Wang, X.; Chen, Z.; Hu, M.; Tian, Y.; Jin, X.; Ma, S.; Xu, T.; Hu, Z.; Liu, S.; Guo, D.; Xiao, B. Chemical Looping Combustion of Biomass Using Metal Ferrites as Oxygen Carriers. *Chem. Eng. J.* **2017**, *312*, 252−262.
(67) Mei, D.; Soleimanisalim, A. H.; Linderholm, C.; Lyngfelt, A.; Mattisson, T. Reactivity and Lifetime Assessment of an Oxygen Releasable Manganese Ore with Biomass Fuels in a 10 KWth Pilot Rig for Chemical Looping Combustion. *Fuel Process. Technol.* **2021**, *215* (October), 106743.
(68) Schmitz, M.; Linderholm, C.; Hallberg, P.; Sundqvist, S.; Lyngfelt, A. Chemical-Looping Combustion of Solid Fuels Using Manganese Ores as Oxygen Carriers. *Energy Fuels* **2016**, *30* (2), 1204−1216.
(69) Schmitz, M.; Linderholm, C. Chemical Looping Combustion of Biomass in 10- and 100-KW Pilots - Analysis of Conversion and Lifetime Using a Sintered Manganese Ore. *Fuel* **2018**, *231* (February), 73−84.
(70) Linderholm, C.; Schmitz, M.; Biermann, M.; Hanning, M.; Lyngfelt, A. Chemical-Looping Combustion of Solid Fuel in a 100 KW Unit Using Sintered Manganese Ore as Oxygen Carrier. *Int. J. Greenhouse Gas Control* **2017**, *65* (July), 170−181.
(71) Pikkarainen, T.; Hiltunen, I. Chemical Looping Combustion of Solid Biomass−Performance of Ilmenite and Braunite as Oxygen Carrier Materials. *In 25th European Biomass Conference and Exhibition*, 2017; pp 12−15.
(72) Moldenhauer, P.; Sundqvist, S.; Mattisson, T.; Linderholm, C. Chemical-Looping Combustion of Synthetic Biomass-Volatiles with Manganese-Ore Oxygen Carriers. *Int. J. Greenhouse Gas Control* **2018**, *71* (March), 239−252.
(73) Pérez-Astray, A.; Mendiara, T.; de Diego, L. F.; Abad, A.; García-Labiano, F.; Izquierdo, M. T.; Adánez, J. Improving the Oxygen Demand in Biomass CLC Using Manganese Ores. *Fuel* **2020**, *274* (December), 117803.
(74) Pérez-Astray, A.; Mendiara, T.; de Diego, L. F.; Abad, A.; García-Labiano, F.; Izquierdo, M. T.; Adánez, J. Behavior of a Manganese-Iron Mixed Oxide Doped with Titanium in Reducing the Oxygen Demand for CLC of Biomass. *Fuel* **2021**, *292* (May), 120381.
(75) Adánez-Rubio, I.; Abad, A.; Gayán, P.; Adánez, I.; De Diego, L. F.; García-Labiano, F.; Adánez, J. Use of Hopcalite-Derived Cu-Mn Mixed Oxide as Oxygen Carrier for Chemical Looping with Oxygen Uncoupling Process. *Energy Fuels* **2016**, *30* (7), 5953−5963.
(76) Niu, Y.; Tan, H.; Hui, S. Ash-Related Issues during Biomass Combustion: Alkali-Induced Slagging, Silicate Melt-Induced Slagging (Ash Fusion), Agglomeration, Corrosion, Ash Utilization, and Related Countermeasures. *Prog. Energy Combust. Sci.* **2016**, *52*, 1−61.
(77) Grimm, A.; Öhman, M.; Lindberg, T.; Fredriksson, A.; Boström, D. Bed Agglomeration Characteristics in Fluidized-Bed Combustion of Biomass Fuels Using Olivine as Bed Material. *Energy Fuels* **2012**, *26* (7), 4550−4559.
(78) Hanning, M.; Corcoran, A.; Lind, F.; Rydén, M. Biomass Ash Interactions with a Manganese Ore Used as Oxygen-Carrying Bed Material in a 12 MWth CFB Boiler. *Biomass Bioenergy* **2018**, *119* (October), 179−190.
(79) Khan, A. A.; de Jong, W.; Jansens, P. J.; Spliethoff, H. Biomass Combustion in Fluidized Bed Boilers: Potential Problems and Remedies. *Fuel Process. Technol.* **2009**, *90* (1), 21−50.

https://doi.org/10.1021/acs.energyfuels.1c02600
Energy Fuels 2021, 35, 19248−19265

(80) Basu, P. *Biomass Gasification, Pyrolysis and Torrefaction: Practical Design and Theory* **2013**, DOI: 10.1016/C2011-0-07564-6.
(81) Gatternig, B.; Karl, J. Investigations on the Mechanisms of Ash-Induced Agglomeration in Fluidized-Bed Combustion of Biomass. *Energy Fuels* **2015**, *29* (2), 931−941.
(82) Gu, H.; Shen, L.; Zhong, Z.; Zhou, Y.; Liu, W.; Niu, X.; Ge, H.; Jiang, S.; Wang, L. Interaction between Biomass Ash and Iron Ore Oxygen Carrier during Chemical Looping Combustion. *Chem. Eng. J.* **2015**, *277*, 70−78.
(83) Scala, F. Particle Agglomeration during Fluidized Bed Combustion: Mechanisms, Early Detection and Possible Countermeasures. *Fuel Process. Technol.* **2018**, *171* (November), 31−38.
(84) Johansen, J. M.; Jakobsen, J. G.; Frandsen, F. J.; Glarborg, P. Release of K, Cl, and S during Pyrolysis and Combustion of High-Chlorine Biomass. *Energy Fuels* **2011**, *25* (11), 4961−4971.
(85) Fatehi, H.; Li, Z. S.; Bai, X. S.; Aldén, M. Modeling of Alkali Metal Release during Biomass Pyrolysis. *Proc. Combust. Inst.* **2017**, *36* (2), 2243−2251.
(86) Hupa, M.; Karlström, O.; Vainio, E. Biomass Combustion Technology Development - It Is All about Chemical Details. *Proc. Combust. Inst.* **2017**, *36* (1), 113−134.
(87) Zevenhoven, M.; Yrjas, P.; Hupa, M. Ash□Forming Matter and Ash□Related Problems. *Handb. Combust. Online* **2010**, 493−531.
(88) Hupa, M. Ash-Related Issues in Fluidized-Bed Combustion of Biomasses: Recent Research Highlights. *Energy Fuels* **2012**, *26* (1), 4−14.
(89) Staničić, I.; Andersson, V.; Hanning, M.; Mattisson, T.; Backman, R.; Leion, H. Combined Manganese Oxides as Oxygen Carriers for Biomass Combustion — Ash Interactions. *Chem. Eng. Res. Des.* **2019**, *149*, 104−120.
(90) Staničić, I.; Hanning, M.; Deniz, R.; Mattisson, T.; Backman, R.; Leion, H. Interaction of Oxygen Carriers with Common Biomass Ash Components. *Fuel Process. Technol.* **2020**, *200* (October), 106313.
(91) Gogolev, I.; Pikkarainen, T.; Kauppinen, J.; Linderholm, C.; Steenari, B. M.; Lyngfelt, A. Investigation of Biomass Alkali Release in a Dual Circulating Fluidized Bed Chemical Looping Combustion System. *Fuel* **2021**, *297* (November), 120743.
(92) Gogolev, I.; Soleimanisalim, A. H.; Linderholm, C.; Lyngfelt, A. Commissioning, Performance Benchmarking, and Investigation of Alkali Emissions in a 10 KWth Solid Fuel Chemical Looping Combustion Pilot. *Fuel* **2021**, *287* (September), 119530.
(93) Cheng, D.; Yong, Q.; Zhao, Y.; Gong, B.; Zhang, J. Study on the Interaction of the Fe-Based Oxygen Carrier with Ashes. *Energy Fuels* **2020**, *34* (8), 9796−9809.
(94) Yilmaz, D.; Leion, H. Interaction of Iron Oxygen Carriers and Alkaline Salts Present in Biomass-Derived Ash. *Energy Fuels* **2020**, *34* (9), 11143−11153.
(95) Zevenhoven, M.; Sevonius, C.; Salminen, P.; Lindberg, D.; Brink, A.; Yrjas, P.; Hupa, L. Defluidization of the Oxygen Carrier Ilmenite − Laboratory Experiments with Potassium Salts. *Energy* **2018**, *148*, 930−940.
(96) Zhang, S.; Xiao, R. Performance of Iron Ore Oxygen Carrier Modified by Biomass Ashes in Coal-Fueled Chemical Looping Combustion. *Greenhouse Gases: Sci. Technol.* **2016**, *6* (5), 695.
(97) Störner, F.; Hildor, F.; Leion, H.; Zevenhoven, M.; Hupa, L.; Rydén, M. Potassium Ash Interactions with Oxygen Carriers Steel Converter Slag and Iron Mill Scale in Chemical-Looping Combustion of Biomass-Experimental Evaluation Using Model Compounds. *Energy Fuels* **2020**, *34* (2), 2304−2314.
(98) Bhui, B.; V, P. Chemical Looping Based Co-Combustion of High Ash Indian Coal and Rice Straw Operating under CO2 in-Situ Gasification Mode. *J. Energy Inst.* **2021**, *94*, 176−190.
(99) Bhui, B.; V, P. Chemical Looping Based Co-Combustion of High Ash Indian Coal and Rice Straw Operating under CO2 in-Situ Gasification Mode. *J. Energy Inst.* **2021**, *94*, 176−190.
(100) Luo, M.; Wang, S.; Wang, L.; Lv, M.; Qian, L.; Fu, H. Experimental Investigation of Co-Combustion of Coal and Biomass Using Chemical Looping Technology. *Fuel Process. Technol.* **2013**, *110*, 258−267.
(101) Bhui, B.; Vairakannu, P. Prospects and Issues of Integration of Co-Combustion of Solid Fuels (Coal and Biomass) in Chemical Looping Technology. *J. Environ. Manage.* **2019**, *231* (January), 1241−1256.
(102) Scala, F.; Solimene, R.; Montagnaro, F. 7−Conversion of Solid Fuels and Sorbents in Fluidized Bed Combustion and Gasification. *Fluidized Bed Technologies for Near-Zero Emission Combustion and Gasification* **2013**, 319−387.
(103) Pragadeesh, K. S.; Regupathi, I.; Sudhakar, D. R. Study of Devolatilization during Chemical Looping Combustion of Large Coal and Biomass Particles. *J. Energy Inst.* **2020**, *93* (4), 1460−1472.
(104) Pragadeesh, K. S.; Sudhakar, D. R. Color Indistinction Method for the Determination of Devolatilization Time of Large Fuel Particles in Chemical Looping Combustion. *Energy Fuels* **2019**, *33* (5), 4542−4551.
(105) Zhang, J. Q.; Becker, H. A.; Code, R. K. Devolatilization and Combustion of Laree Coal Particles in a Fluidized Bed. *Can. J. Chem. Eng.* **1990**, *68*, 1010−1017.
(106) Stubington, J. F.; Linjewile, T. M. The Effects of Fragmentation on Devolatilization of Large Coal Particles. *Fuel* **1989**, *68* (2), 155−160.
(107) Ross, D. P.; Heidenreich, C. A.; Zhang, D. K. Devolatilisation Times of Coal Particles in a Fluidised-Bed. *Fuel* **2000**, *79* (8), 873−883.
(108) Solimene, R.; Chirone, R.; Salatino, P. Characterization of the Devolatilization Rate of Solid Fuels in Fluidized Beds by Time-Resolved Pressure Measurements. *AIChE J.* **2012**, *58* (2), 632.
(109) Haus, J.; Lindmüller, L.; Dymala, T.; Jarolin, K.; Feng, Y.; Hartge, E. U.; Heinrich, S.; Werther, J. Increasing the Efficiency of Chemical Looping Combustion of Biomass by a Dual-Stage Fuel Reactor Design to Reduce Carbon Capture Costs. *Mitig. Adapt. Strateg. Glob. Chang.* **2020**, *25* (6), 969−986.
(110) Thon, A.; Kramp, M.; Hartge, E. U.; Heinrich, S.; Werther, J. Operational Experience with a System of Coupled Fluidized Beds for Chemical Looping Combustion of Solid Fuels Using Ilmenite as Oxygen Carrier. *Appl. Energy* **2014**, *118*, 309−317.
(111) Scala, F.; Chirone, R.; Salatino, P. 6−Attrition Phenomena Relevant to Fluidized Bed Combustion and Gasification Systems. *Woodhead Publishing Series in Energy* **2013**, 254−315.
(112) Pragadeesh, K. S.; Sudhakar, D. R. Primary Fragmentation Behavior of Indian Coals and Biomass during Chemical Looping Combustion. *Energy Fuels* **2018**, *32* (5), 6330−6346.
(113) Pragadeesh, K. S.; Regupathi, I.; Ruben Sudhakar, D. Insitu Gasification − Chemical Looping Combustion of Large Coal and Biomass Particles: Char Conversion and Comminution. *Fuel* **2021**, *292* (January), 120201.
(114) Zheng, Y.; Grant, R.; Hu, W.; Scott, S. A. Pyrolysis of Wood Pellets in the Presence of Oxygen Carriers in a Fluidised Bed Coupled with a DBD Reactor for Tar Quantification. *Chem. Eng. J.* **2019**, *355* (August), 858−870.
(115) Boot-Handford, M. E.; Florin, N.; Fennell, P. S. Investigations into the Effects of Volatile Biomass Tar on the Performance of Fe-Based CLC Oxygen Carrier Materials. *Environ. Res. Lett.* **2016**, *11* (11), 115001.
(116) Pérez-Astray, A.; Adánez-Rubio, I.; Mendiara, T.; Izquierdo, M. T.; Abad, A.; Gayán, P.; de Diego, L. F.; García-Labiano, F.; Adánez, J. Comparative Study of Fuel-N and Tar Evolution in Chemical Looping Combustion of Biomass under Both IG-CLC and CLOU Modes. *Fuel* **2019**, *236* (August), 598−607.
(117) Zhou, L.; Deshpande, K.; Zhang, X.; Agarwal, R. K. Process Simulation of Chemical Looping Combustion Using ASPEN plus for a Mixture of Biomass and Coal with Various Oxygen Carriers. *Energy* **2020**, *195*, 116955.
(118) Yin, W.; Wang, S.; Zhang, K.; He, Y. Numerical Investigation of in Situ Gasification Chemical Looping Combustion of Biomass in a Fluidized Bed Reactor. *Renewable Energy* **2020**, *151*, 216−225.

(119) Kevat, M. D.; Banerjee, T. Process Simulation and Energy Analysis of Chemical Looping Combustion and Chemical Looping with Oxygen Uncoupling for Sawdust Biomass. *Energy Technol.* **2018**, *6* (7), 1237−1247.
(120) Zylka, A.; Krzywanski, J.; Czakiert, T.; Idziak, K.; Sosnowski, M.; de Souza-Santos, M. L.; Sztekler, K.; Nowak, W. Modeling of the Chemical Looping Combustion of Hard Coal and Biomass Using Ilmenite as the Oxygen Carrier. *Energies* **2020**, *13* (20), 5394.
(121) Hamidouche, Z.; Ku, X.; Lin, J.; Wang, J. Numerical Simulation of a Chemical Looping Combustion of Biomass: Hydrodynamic Investigation. *Fuel Process. Technol.* **2020**, *207* (June), 106486.
(122) Abad, A.; Mendiara, T.; de Diego, L. F.; García-Labiano, F.; Gayán, P.; Adánez, J. A Simple Model for Comparative Evaluation of Different Oxygen Carriers and Solid Fuels in IG-CLC Processes. *Fuel Process. Technol.* **2018**, *179* (June), 444−454.
(123) Situmorang, Y. A.; Zhao, Z.; An, P.; Rizkiana, J.; Prakoso, T.; Abudula, A.; Guan, G. A Small-Scale Power Generation System Based on Biomass Direct Chemical Looping Process with Organic Rankine Cycle. *Chem. Eng. Process.* **2021**, *163* (September), 108361.
(124) Sikarwar, S. S.; Surywanshi, G. D.; Patnaikuni, V. S.; Kakunuri, M.; Vooradi, R. Chemical Looping Combustion Integrated Organic Rankine Cycled Biomass-Fired Power Plant − Energy and Exergy Analyses. *Renewable Energy* **2020**, *155*, 931−949.
(125) EU Biomass Availability and Sustainability Information System. *Report on Conversion Efficiency of Biomass*; 2015.
(126) Chein, R. Y.; Chen, W. H. Thermodynamic Analysis of Integrated Adiabatic Chemical Looping Combustion and Supercritical CO2 Cycle. *Energy Convers. Manag. X* **2021**, *10* (February), 100078.
(127) Bareschino, P.; Mancusi, E.; Urciuolo, M.; Coppola, A.; Solimene, R.; Pepe, F.; Chirone, R.; Salatino, P. Modelling of a Combined Biomass CLC Combustion and Renewable-Energy-Based Methane Production System for CO2 Utilization. *Powder Technol.* **2020**, *373*, 421−432.
(128) Mancusi, E.; Bareschino, P.; Brachi, P.; Coppola, A.; Ruoppolo, G.; Urciuolo, M.; Pepe, F. Feasibility of an Integrated Biomass-Based CLC Combustion and a Renewable-Energy-Based Methanol Production Systems. *Renewable Energy* **2021**, *179*, 29−36.
(129) Lindroos, T. J.; Rydén, M.; Langørgen, Ø.; Pursiheimo, E.; Pikkarainen, T. Robust Decision Making Analysis of BECCS (Bio-CLC) in a District Heating and Cooling Grid. *Sustain. Energy Technol. Assessments* **2019**, *34* (December), 157−172.
(130) Keller, M.; Kaibe, K.; Hatano, H.; Otomo, J. Techno-Economic Evaluation of BECCS via Chemical Looping Combustion of Japanese Woody Biomass. *Int. J. Greenhouse Gas Control* **2019**, *83* (February), 69−82.
(131) Haaf, M.; Ohlemüller, P.; Ströhle, J.; Epple, B. Techno-Economic Assessment of Alternative Fuels in Second-Generation Carbon Capture and Storage Processes. *Mitig. Adapt. Strateg. Glob. Chang.* **2020**, *25* (2), 149−164.

https://doi.org/10.1021/acs.energyfuels.1c02600
Energy Fuels 2021, 35, 19248−19265